Influence of atmospheric deposition on biogeochemical cycles in an oligotrophic ocean system

France Van Wambeke¹, Vincent Taillandier², Karine Desboeufs³, Elvira Pulido-Villena¹, Julie Dinasquet^{4,5}, Anja Engel⁶, Emilio Marañón⁷, Céline Ridame⁸, Cécile Guieu²

5

¹ Aix-Marseille Université, CNRS/INSU, Université de Toulon, IRD, Mediterranean Institute of Oceanography (MIO) UM 110, 13288, Marseille, France

² CNRS, Sorbonne Université, Laboratoire d'Océanographie de Villefranche (LOV), UMR7093, 06230 Villefranche-sur-Mer, France

10 ³LISA, UMR CNRS 7583, Université Paris-Est-Créteil, Université de Paris, Institut Pierre Simon Laplace (IPSL), Créteil, France

⁴ Sorbonne Universités, Laboratoire d'Océanographie Microbienne (LOMIC), Observatoire Océanologique, 66650, Banyuls/mer, France

⁵ Marine Biology Research Division, Scripps Institution of Oceanography, UCSD, La Jolla, USA

 ⁶ GEOMAR – Helmholtz-Centre for Ocean Research, Kiel, Germany
 ⁷ Department of Ecology and Animal Biology, Universidade de Vigo, 36310 Vigo, Spain
 ⁸ Sorbonne University/CNRS/IRD/MNHN, LOCEAN: Laboratoire d'Océanographie et du Climat: Expérimentation et Approches Numériques, UMR 7159, 4 Place Jussieu – 75252 Paris Cedex 05, France

The surface mixed layer (ML) in the Mediterranean Sea is a well stratified domain

Correspondence to: France Van Wambeke (france.van-wambeke@mio.osupytheas.fr) and

20 Cécile Guieu (guieu@imev-mer.fr)

Abstract.

25

characterized by low macro-nutrients and low chlorophyll content, for almost 6 months of the year. In this study we characterize the biogeochemical cycling of <u>nitrogen (N)</u> in the ML by analysing simultaneous *in situ* measurements of atmospheric deposition, nutrients <u>in seawater</u>, hydrological conditions, primary production, heterotrophic prokaryotic production, N₂ fixation and leucine aminopeptidase activity. Dry deposition was continuously measured across the central and western open Mediterranean Sea and two wet deposition events were

sampled, one in the Ionian Sea and one in the Algerian <u>Basin</u>. Along the transect, N budgets were computed to compare the sources and sinks of N in the mixed layer. *In situ* leucine aminopeptidase activity made up 14 to 66 % of the heterotrophic prokaryotic N demand, and the N_2 fixation rate represented 1 to 4.5 % of the phytoplankton N demand. Dry atmospheric Supprimé: basin

³⁰

40

- deposition of inorganic nitrogen, estimated from dry deposition of (nitrate and ammonium) in aerosols, was higher than the N_2 fixation rates in the ML (on average 4.8-fold). The dry atmospheric input of inorganic N represented a highly variable proportion of biological N demand in the ML among the stations, 10 - 82% for heterotrophic prokaryotes and 1-30% for phytoplankton. As some sites were visited <u>during</u> several days the evolution of biogeochemical properties in the ML and within the nutrient-depleted layers could be followed. At the Algerian Basin site, the biogeochemical consequences of a wet dust
- deposition event wre monitored by a high frequency sampling of CTD casts. Notably just after the rain, nitrate was higher in the ML than in the nutrient depleted layer below. Estimates of nutrient transfer from the ML into the nutrient depleted layer could explain up to a ¹/₃ of the nitrate loss from the ML. Phytoplankton did not benefit directly from the atmospheric inputs
- into the ML, probably due to high competition with heterotrophic prokaryotes, also limited by
 N and <u>phosphorus (P)</u> availability at the time of this study. Primary producers decreased their
 production after the rain, <u>they recovered</u> their initial state of activity after a 2-day lag in the
 vicinity of the deep chlorophyll maximum layer.

50 1. Introduction

The Mediterranean Sea (MS) is a semi-enclosed basin characterized by <u>active</u> ventilation and <u>short</u> residence times <u>of the newly formed waters</u>, due to its own thermohaline circulation (Mermex Group, 2011). In terms of biogeochemistry, the MS is <u>characterized by a long</u> <u>summer stratification period</u>, a west-to-east gradient of jncreasing oligotrophy, and a deficit in

55 phosphorus (P) compared to nitrogen (Mermex Group, 2011). The last feature is confirmed by a deep N/P ratio for inorganic nutrients higher than the Redfield ratio that increases toward the east (Krom et al., 2004).

The relationship between photoautotrophic unicellular organisms and heterotrophic prokaryotes (competition or commensalism) is affected by the balance of light and nutrients

- as well as possible inputs of organic matter from river runoff or atmospheric deposition.
 Phytoplankton generally experience P, or N limitation, or both (Thingstad et al., 2005; Tanaka et al., 2011, Richon et al., 2018), whereas heterotrophic prokaryotes are usually P
 limited, or P and organic carbon co-limited (Sala et al., 2002, Van Wambeke et al., 2002, Céa et al., 2014).
- 65 The MS <u>continuously</u> receives anthropogenic aerosols, originating from industrial and domestic activities from around the basin and from other parts of Europe₁ along with pulsed

Supprimé: +

Supprimé: for

Supprimé: was followed Supprimé: with

Supprimé: P
Supprimé: recovering
Supprimé: to
Supprimé:

Supprimé: very short

Supprimé: is characterized by a long summer stratification period. It Supprimé: Supprimé: a low nutrient, low chlorophyll (LNLC) system with where there is generallly an increasing oligotrophic gradient Supprimé: from west to eas Supprimé: t Supprimé: and Supprimé: n overall Supprimé: (N) Supprimé: is is Supprimé: n Supprimé: that is Supprimé: in deep layers, Supprimé: which Supprimé: , or Supprimé: NP Supprimé: labile Supprimé: continuously

natural inputs from the Sahara. It is thus a natural LNLC study area, well adapted to investigate the role of ocean–atmosphere exchanges of particles and gases on marine biogeochemical cycles. Recent studies describe annual records of atmospheric deposition of

- trace metals and inorganic macronutrients (N, P) obtained at several locations around the MS
 (Markaki et al., 2010; Guieu and Ridame, in press; Desboeufs, in press). All records <u>show</u>
 pulsed and highly variable <u>atmospheric</u> inputs. Recent models and observations show that
 atmospheric deposition of organic matter (OM) is also highly variable and that their annual
 inputs are of the same order of magnitude as river inputs (Djaoudi et al., 2017, Kanakidou et
- al., 2018; Kanakidou et al., 2020; Galetti et al., 2020). Moreover, the sum of atmospheric inputs of nitrate, ammonium and soluble organic nitrogen has been shown to be equivalent or higher than those of N₂ fixation rates (Sandroni et al., 2007), although inorganic atmospheric N inputs alone may also be higher than N₂ fixation rates (Bonnet et al., 2011).
 Aerosol amendments in bottles, minicosms or mesocosms have been widely used to study
- trophic transfer and potential export, as they <u>allow natural communities to be studied under</u> <u>controlled conditions</u> (i.e. Guieu et al., 2010; Herut et al., 2016; Mescioglu et al., 2019). <u>Both</u> diversity and functioning of various biological compartments are impacted by aerosol additions in different waters tested in the MS (Guieu and Ridame, in press, and Figure 3 therein). Differences in the biological responses have been observed, depending on the mode
- 115 of deposition simulated (wet or dry), the type of aerosols used (natural or anthropogenic) and the *in situ* biogeochemical conditions at the time of the experiment (Guieu and Ridame, in press).

Organic carbon from aerosols is partly soluble, and this soluble fraction is partly available to marine heterotrophic prokaryotes (Djaoudi et al., 2020). Heterotrophic prokaryotes have the
 metabolic capacity to respond quickly to aerosol deposition through growth and changes in community composition (Rahav et al., 2016; Pulido-Villena et al., 2008; 2014), while the phytoplankton community responds more slowly or not at all (Guieu and Ridame, in press, and reference therein).

Owing to the intrinsic experimental limitations, which vary depending on the size and design of enclosures (i.e. the omission of higher trophic levels, absence of turbulent mixing so limiting exchanges by diffusion, and wall effects) such experiments cannot, however, fully simulate *in situ* conditions (Guieu and Ridame, in press). Thus, *in situ* observations <u>are</u> <u>required</u> to understand the consequences of aerosol deposition on biogeochemical cycling in the world's ocean. Such *in situ* studies are scarce and require dedicated, high-frequency **Supprimé:** Parameterization and representation of the key processes brought into play by atmospheric deposition in the MS must take into account the role of pulsed atmospheric inputs (Guieu et al., 2014a).

Supprimé: denote

Supprimé: the

Supprimé: represent to some extent a 'simplified' plankton trophic web that can Supprimé: along a vertical dimension Supprimé: It has been shown that b

Supprimé: synthesis

Supprimé: it is still necessary to acquire
Supprimé: es

Supprimé:

sampling to follow the effects of deposition on the biogeochemical processes while taking into account the water column dynamics as recently emphasized in cases studies (Pulido-Villena et al., 2008 and Rahav et al., 2016),

Hence, there is a need for sampling surveys with adaptive strategies to follow aerosol

- deposition events *in situ* and their impacts on biogeochemical processes, especially in the open waters of the stratified and nutrient limited MS. The objectives of the PEACETIME project were to study fundamental processes and their interactions at the ocean–atmosphere interface following atmospheric deposition (especially of Saharan dust) in the Mediterranean Sea, and how these processes impact the functioning of the pelagic ecosystem (Guieu et al., 2000).
- 155 2020).

As atmospheric deposition affects primarily the surface mixed layer (ML), the present study focuses on the upper part of the nutrient depleted layer that extends down to the nutriclines (as defined by Du et al., 2017). During the stratification period, concentrations of nitrate and phosphate inside the ML are often below the <u>detection</u> limits of standard methods. However,

nanomolar concentrations of nitrate (and phosphate) can now be assessed accurately through the Long Waveguide Capillary Cell (LWCC) technique (Zhang and Chi, 2002), which permits the measurement of fine gradients inside nutrient depleted layers of the MS (Djaoudi et al., 2018).

The aims of the present study were to assess the impact of atmospheric nutrient deposition on biogeochemical processes and fluxes in the open sea during the PEACTIME cruise in the MS. For this, i) we estimated nanomolar variations of nitrate concentration, in the surface mixed layer (ML) <u>under</u> variable inputs of dry and wet aerosol deposition and ii) we compared the aerosol-derived N inputs to the ML with biological activities: primary production,

heterotrophic prokaryotic production, N₂ fixation and ectoenzymatic (leucine aminopeptidase)
 activity. We studied the N budgets along a zonal transect that includes 13 stations crossing the
 Algerian Basin, Tyrrhenian Sea and the Ionian Sea where dry atmospheric deposition was

- continuously measured on board together with seawater biogeochemical, biological and physical characteristics. We finally focused on a wet deposition event that occurred in the western Algerian Basin, where we investigated the evolution of biogeochemical fluxes of
- both N and P and microbial activities through the high frequency sampling.

2. Materials and Methods

2.1 Sampling strategy and measured parameters

Supprimé: To demonstrate this point, the biological response to a Saharan dust event (dust flux = 2.6 g m⁻² recorded at a coastal station in Cap Ferrat) was detected 4 days after the event by only one offshore water column sampling (at the DYFAMED site). An increase in heterotrophic prokaryotic respiration and abundance was observed when compared to a sampling that was carried out 16 days before this dust event (Pulido-Villena et al., 2008)

Supprimé: Off the Israelian coast a moderate natural dust storm (1.05 mg L⁻¹ over 5 m depth) was followed every 12 hours over 5 days (Rahav et al., 2016). Rapid changes were observed, which could have been missed without high frequency sampling. A decrease in picophytoplankton abundance, an increase in heterotrophic prokaryote abundance, as well as a slight increase in primary production (25%) and heterotrophic prokaryotic production (15%) was observed.¶

Supprimé: it is necessary to organize Supprimé: quantification

Supprimé: we	
Supprimé: s	
Supprimé: facing	
Supprimé: activity	
Suppline: activity	
Supprimé: ,	
Supprimé: o	

Supprimé: high frequency sampling of a

The PEACETIME cruise (doi.org/10.17600/15000900) was conducted in the Mediterranean Sea, from May to June 2017, along a transect extending from the Western Basin to the center of the Ionian Sea (Fig. 1). For details on the cruise strategy, see Guieu et al. (2020). Short duration stations (< 8 h, 10 stations named ST1 to ST10, Fig. 1) and long duration sites (5

- 215 days, 3 sites named TYR, ION and FAST) were occupied. Chemical composition of aerosols was quantified by continuous sampling along the whole transect. In addition, two rain events were sampled (Desboeufs et al., this issue, in prep.), one on the 29th of May at ION site, and a second one, a dust wet deposition event, at FAST site on the 5th of June.
- At least 3 CTD casts were conducted at each short station. One cast focused on the epipelagic 220 layer (0-250 m), another on the whole water column. Two were carried out with a standard, CTD rosette equipped with 24 Niskin bottles (12 L), and a Sea-Bird SBE9 underwater unit with pressure, temperature (SBE3), conductivity (SBE4), chlorophyll fluorescence (Chelsea Acquatracka) and oxygen (SBE43) sensors. A third cast, from the surface to the bottom of the water column was <u>carried out</u> under trace metal clean conditions using instrumental package 225 including a titanium rosette (hereafter TMC-rosette) mounted on a Kevlar cable and equipped with Go-Flo bottles that were sampled in a dedicated clean lab container. The long duration sites were abbreviated as TYR (situated in the center of the Tyrrhenian Basin), ION (in the center of the Ionian Basin), and FAST (in the western Algerian Basin). These 3 sites were selected based on satellite imagery, altimetry and Lagrangian diagnostics as well as forecasted 230 rain events (Guieu et al., 2020). At these sites, repeated casts were performed over at least 4 days with alternating CTD- and TMC- rosettes (Table 1). The succession of CTD casts at the FAST site is numbered in days relative to a rain event <u>sampled</u> on board the ship. The first cast of the series was sampled 2.3 days before the rain event, and the last 2 days after. The FAST site was revisited following the study at ST10 (3.8 days after the rain event). 235 Primary production (PP), prokaryotic heterotrophic production (BP), heterotrophic prokaryotic abundances (hprok), ectoenzymatic activities (leucine aminopeptidase (LAP) and alkaline phosphatase (AP)), were determined on water samples collected with the standard CTD-rosette. Dissolved inorganic nutrients, dissolved organic nitrogen (DON) and phosphorus (DOP) were measured on water samples collected using the TMC-rosette. LAP and AP were determined from two layers in the epipelagic waters (5 m depth and deep 240 chlorophyll maximum (DCM)) at the short stations and at the ION and TYR sites In addition,

LAP and AP were determined at 4 depths between 0 and 20 m for 4 profiles at FAST site, to

determine the variability within the ML.

Supprimé: Both of these
Supprimé: sampled
Supprimé: classical-
Supprimé: a sampling system of
Supprimé: equipped
Supprimé: performed
Supprimé: '
Supprimé: '
Supprimé: a second
Supprimé: called
Supprimé: ,
Supprimé: using
Supprimé: and
Supprimé: minimum of
Supprimé: ;
Supprimé: collected

Supprimé: of

Supprimé: classical

Supprimé: get insight on

2.2 Analytical methods and fluxes calculations

265 2.2.1 Nutrients in the atmosphere

	Total suspended aerosol particles (TSP inlet) were collected continuously throughout the	Supprimé: For dry deposestimations, the t
	campaign for dry deposition estimations. Aerosol sampling was carried out using filtration	Supprimé: accomplished
	units on adapted membranes for off-line chemical analysis (Tovar-Sanchez et al., 2020).	Supprimé: by
	Simultaneously, water soluble fraction of the aerosols was sampled continuously, using a	Supprimé: In parallel to filter sampling
270	Particle-into-Liquid-Sampler (PILS, Orsini et al., 2003). Moreover, two wet deposition events	Supprimé: s
	were sampled, one at the ION site, one at the FAST site using rain collectors with on-line	Supprimé: on board the
	filtration (porosity 0.2 μ m) (details in Desbeoufs et al., this issue, in prep)	cruise
	Nitrate and ammonium concentrations in the aerosols, abbreviated in the text as NO3 and	Supprimé: The n
	NH4 respectively, were analyzed continuously on board from May 13 th , using PILS sampling	Supprimé: toNO3
275	coupled on-line with double way ion chromatography (PILS-IC, Metrohm, model 850	Supprimé: (nitrite conce under analytical detection l
	Professional IC with Metrosep A Supp 7 column for anion measurements and Metrosep C4	
	column for cation measurements). The <u>temporal</u> resolution for PILS-IC analysis was 70 min,	Supprimé: time
	for anions and 32 min for cations. Dissolved Inorganic Nitrogen (DIN) fluxes released by dry	Supprimé: .
	deposition were estimated by multiplying NO3 and NH4 obtained through PILS-CI	Supprimé: from the
• • • •		Supprimé: the
280	measurements (nitrite concentrations were under analytical detection limits) by the dry	Supprimé: by
	settling velocities of N-bearing aerosols, i.e 0.21 and 1 cm s ⁻¹ for NH4 and NO3, respectively	
	(Kouvarakis et al., 2001). Mean <u>NO3 and NH4</u> concentrations were <u>calculated</u> from the PILS-	Supprimé: used
	IC data measured (1) during the occupation of each short station lasting between 0.13 and	Supprimé: which were
	0.66 days (with on average 5 measurements for NO3 and 11 measurements for NH4), and (2)	Supprimé: at
285	between two successive casts at the sites with a time lag between 0.4 and 1.21 days (with on	Supprimé: i.e. enabling
205		Supprimé: in
	average 15 measurements for NO3 and about 30 for NH4). At ST1, NH4 and NO3	Supprimé: of Supprimé: to1
	concentrations were obtained using IC analyses following water extraction from aerosol filter	Supprimé: i.e. enabling
	sampling as the PILS-IC was not operational.	(
	Total dissolved phosphate (TDP) concentrations were estimated from soluble P	
290	concentrations extracted from particulate aerosols collected on filters after ultrapure water	Supprimé: under
	extraction HR-ICP-MS analysis (Neptune Plus, Thermo Scientific ™) (Fu et al., this issue, in	Supprimé: using
		Supprimé: DIN
	prep) since it was generally <u>below the detection limits of the PILS-IC technique. The</u>	Supprimé: :
	frequency of TDP analysis was therefore less than for NO3 and NH4 (0.28 -1.15 days	Supprimé: the filters san duration of the short station
	depending on the stations). At the JON, TYR and FAST sites, filters collected aerosols at	Supprimé: 3
295	different periods including each CTD cast, when possible.	Supprimé: during
		Supprimé: s sampling da

position ned to the total aerosol he ship during the centrations were

under	anal	ytical	detec	tion 1	imits)	

Supprimé: time
Supprimé:
Supprimé: from the
Supprimé: the
Supprimé: by

Supprimé: under
Supprimé: using
Supprimé: DIN
Supprimé: :
Supprimé: the filters sampled over the duration of the short station
Supprimé: 3
Supprimé: during
Supprimé: s sampling date

	Atmospheric deposition of soluble P was estimated by multiplying the TDP concentration by
	a dry settling velocity of 1 cm s ⁻¹ , except at the FAST site, where 3 cm s ⁻¹ , was used as this
	value is better adapted for lithogenic particles (Izquierdo et al., 2012). The dissolved fraction
	and solution from digestion (Heimburger et al., 2012) of particulate fractions in the filters
335	were analysed by ICP-AES (Inductively Coupled Plasma Atomic Emission Spectrometry,
	Spectro ARCOS Ametek®). The speciation organic/inorganic of TDP was determined from
	ICP-MS and IC analysis. DOP was estimated from the difference between TDP, obtained by
	ICP-MS, and DIP, obtained by ion chromatography.

- In the rain samples, NO3, NH4 and dissolved inorganic phosphorus (DIP) were also determined using ion chromatography following recovery of the dissolved fraction, <u>Total</u> <u>particulate P (TPP) and dissolved organic P (DOP) were also measured in the rain samples</u> following a similar protocol used for atmospheric dust (described above). The wet deposition fluxes of <u>dust dissolved</u> nutrients and <u>particulate fractions</u> were estimated from the measured concentrations in the <u>rain sample</u>, multiplied by total precipitation.
- Total precipitation was taken from the total hourly precipitation accumulated during the rain
 event over the region from the ERA5 hourly data reanalysis (Hersbach et al., 2018). In order
 to incorporate the regional variability of rainfall, the total precipitation was taken from the
 total hourly precipitation over a domain whose center is the ship and whose radius measures
 110 km using the ERA5 hourly data reanalysis (Hersbach et al., 2018). ERA 5 data are available on
 regular latitude-longitude grids at 0.25° x 0.25° resolution (Desboeufs et al., in prep., Table 3).
 Cumulative precipitation was obtained by considering the value at the center of each grid
 point over the domain.,

2.2.2 Nutrients in the water column

- Seawater samples for standard nutrient analysis were filtered online (< 0.2 μm, Sartorius
 Sartrobran-P-capsule with a 0.45 μm prefilter and a 0.2 μm final filter) directly from the Go_ FLo bottles (TMC-rosette). Samples collected in acid-washed polyethylene bottles were
 immediately analyzed on board. Micromolar <u>concentrations of nitrate + nitrite (NOx) and DIP</u> were determined using a segmented flow analyzer (AAIII HR SealAnalytical©) following
- Aminot and Kérouel (2007) with a limit of quantification (calculated as ten times the standard deviation of ten measurements of the blank) of 0.050 μM for NOx and 0.020 μM for DIP.
 Samples for the determination of nanomolar concentrations of dissolved nutrients were collected in HDPE bottles previously cleaned with supra-pure HCl. For NOx (primarily NO3)

Supprimé: flux
Supprimé: . A
Supprimé: a
Supprimé: velocity

Supprimé: ¶

Mis en forme : Couleur de police : Automatique Supprimé: , Supprimé: collected onboard the ship,

Supprimé:

Supprimé: in the samples

Supprimé: these

Supprimé: then

Supprimé: dissolved fractions

Supprimé: from the rain samples

Supprimé: Total precipitation was obtained by adding the hourly rainfall onto the grid-points $(0.25^{\circ} \times 0.25^{\circ})$ spanning the ship location, more or less 1° around this central grid-point for integrating the regional variability

Supprimé: (

Supprimé: In the rain samples, total particulate P (TPP) and dissolved organic P (DOP) were also

Supprimé: available. The dissolved fraction and solution from digestion (Heimburger et al., 2012) of particulate fractions in the filters were analysed by ICP-AES (Inductively Coupled Plasma Atomic Emission Spectrometry, Spectro ARCOS Ametek®) for total particulate TPP. The speciation organic/inorganic of TDP was determined from ICP-MS and IC analysis. DOP was estimated from the difference between TDP, obtained by ICP-MS, and DIP, obtained by ion chromatography. ¶

Supprimé:

Supprimé: considered as

I	as the nitrite fraction was mostly negligible), samples were acidified to pH 1 inside the clean	
	<u>container</u> and analyzed back in the laboratory using a spectrometric method in the visible (540	Supprimé: van
	nm), with a 1 m LWCC (Louis et al., 2015). The detection limit was 6 nM, the limit of	Supprimé: limit of
405 I	quantification was 9 nM and the reproducibility was 8.5%. DIP was analyzed immediately	
	after sampling using the LWCC method after Pulido-Villena et al. (2010), with a detection	Supprimé: limit of
	limit of 1 nM (Pulido-Villena et al., 2021). Total dissolved phosphorus (TDP) and nitrogen	
I	(TDN) were measured using the segmented flow analyzer technique after high-temperature	
	(120 °C) persulfate wet oxidation mineralization (Pujo-Pay and Raimbault, 1994). DOP	
410	(DON) was obtained as the difference between TDP (TDN) and DIP (NOx). Labile DOP (L-	
	DOP) was <u>estimated</u> as 31% of the DOP values (Pulido-Villena et al., 2021).	Supprimé: determined
I	Total hydrolysable amino acids (TAAs) were determined as described in detail in Van	Supprimé: this issue, in prep.
	Wambeke et al. (2021). Briefly 1 ml of sample was hydrolyzed at 100°C for 20 h with 1 ml of	
	30% HCl and then neutralized by acid evaporation. Samples were analyzed by high	
415	performance liquid chromatography in duplicate according to Dittmar et al. (2009) protocols.	
	2.2.3 Biological stocks and fluxes in the epipelagic waters	
	Flow cytometry was used for the enumeration of autotrophic prokaryotic and eukaryotic cells,	
	heterotrophic prokaryotes (hprok) and heterotrophic nanoflagellates (HNF). Water samples	Supprimé: Sub
20	(4.5 mL) were fixed with glutaral dehyde grade I 25% (1% final concentration), flash frozen	
	and stored at -80 °C until analysis. Counts were performed on a FACSCanto II flow	
	cytometer (Becton Dickinson). The separation of different autotrophic populations was based	
	on their scattering and fluorescence signals according to Marie et al. (2000). For the	
	enumeration of hprok (Gasol and Del Giorgio, 2000), cells were stained with SYBR Green I	
25	(Invitrogen – Molecular Probes). HNF staining was performed with SYBR Green I as	
	described in Christaki et al. (2011). All cell abundances were determined from the flow rate,	
	which was <u>calibrated</u> with TruCount beads (BD biosciences).	Supprimé: calculated
l	Particulate primary production (PP) was determined at 6 layers from the shallow CTD casts	
	(0-250 m) sampled before sun rise. Samples were inoculated with ¹⁴ C-bicarbonate and	
430	incubated in on-deck incubators kept at in situ temperature by flowing surface seawater and	Supprimé: refrigerated
I	equipped with various blue screens to simulate different irradiance levels. After 24 h-	Supprimé: using running
	incubations, samples were filtered through 0.2 polycarbonate filters and treated for liquid	
	scintillation measurement as described in detail in Marañón et al. (2021). A temperature	
	semination incustrement as described in detail in Warahon et al. (2021). It temperature	

correction was applied as explained in Marañón et al. (2021). N₂ fixation rates (N2fix) were determined as described in Ridame et al. (2011) using 2.3 L of unfiltered seawater <u>collected</u> in acid-washed polycarbonate bottles, and enriched with ¹⁵N2 gas (99 atom% 15N) to obtain a final enrichment of about 10 atom% excess. 24 h-incubations for N2fix were conducted under the same temperature and irradiance as the corresponding PP incubations.

To calculate heterotrophic prokaryotic production (BP) samples collected in the epipelagic layers (0-250 m) were incubated with tritiated leucine using the microcentrifuge technique as detailed in Van Wambeke et al. (2021). We used the empirical conversion factor of 1.5 ng C per pmol of incorporated leucine according to Kirchman (1993). Isotope dilution was negligible under these saturating concentrations as periodically checked with concentration kinetics. As we only used 2 on board temperature controlled dark-incubators, a temperature correction was applied as explained in Van Wambeke et al. (2021). Ectoenzymatic activities
were measured fluorometrically, using the fluorogenic model substrates L-leucine-7-amido-4-methyl-coumarin (Leu-MCA) and 4-methylumbelliferyl-phosphate (MUF-P) to track aminopeptidase (LAP), and alkaline phosphatase (AP), activity, respectively, as described in Van Wambeke et al. (2021). Briefly, the release of MCA from Leu-MCA and MUF from

MUF-P were followed by measuring the increase of fluorescence in the dark (exc/em 380/440 nm for MCA and 365/450 nm for MUF, wavelength width 5 nm) in a VARIOSCAN LUX microplate reader. Fluorogenic substrates were added at varying concentrations in 2 ml wells
(0.025, 0.05, 0.1, 0.25, 0.5 and 1 μM) in duplicate. The parameters Vm (maximum hydrolysis velocity) and Km (Michaelis-Menten constant that reflects enzyme affinity for the substrate) as well as their corresponding errors were estimated by non-linear regression using the

465 <u>Michaelis-Menten</u> equation:

 $V = Vm \times S/(Km + S)$

where V is the hydrolysis rate and S the fluorogenic substrate concentration added. <u>LAP and</u> <u>AP *in situ* activitieswere determined substituting S by</u> TAA and L-DOP <u>in Michaelis-Menten</u> equations, <u>respectively</u> (Van Wambeke et al., 2021; Pulido-Villena et al, 2021).

470

445

2.3. Vertical nutrient fluxes,

In the absence of concomitant turbulence measurements, the mixed layer depth (MLD) <u>can be</u> estimated <u>from density</u> profiles (e.g. de Boyer Montegut et al., 2004; D'Ortenzio et al., 2005), For this study, a MLD was determined <u>at every CTD cast</u> as the depth where the residual Supprimé: (Supprimé:)

Supprimé: ndeed, i Supprimé: hat were Supprimé: , activity Supprimé: , activity Supprimé: From the varying velocities obtained, we determined t Supprimé: fitting the data using a Supprimé: following Supprimé: were then used as substrates to determine LAP and AP *in situ* activities using Supprimé: , Supprimé: .

Supprimé: Vertical partition of the epipelagic layer

Supprimé: ¶

Supprimé: The ML can be in a state of stirring and the density and seawater properties are homogeneous, or in a state of rest with homogeneous density but it is the vertical variations in the non-conservative components (such as nutrients); dependent on momentum and heat fluxes at the interface with the atmosphere, that determine the strength and vertical extent of the mixing (Brainerd and Gregg, 1995).

Supprimé: In this study, with

Supprimé: was

Supprimé: indirectly using the shape of CTD

Supprimé: Classical methods to evaluate MLD from CTD profiles are based on thresholds of the vertical density gap

Supprimé: or on the vertical extension of fixed buoyancy content (Moutin and Prieur, 2012). As discussed in Gardner et al. (1995), the choice of criterion is sensitive to the subtle changes from active mixing to rest, with consequences for the representative time scales of the MLD estimates. In this study, the ML was shallow (10 - 20 m), rapidly activated by the mechanical effects of the wind, and sampled at high frequency (some hours at long duration stations). An approach based on buoyancy criterion has been preferred to resolve short term fluctuations in the mixing state

Supprimé: ,

Supprimé: and

(ML) lead to the formation of a nutrient depleted layer that extend below the ML. Hereafter, the nutrient depleted layer is referred to 'NDLb' (b for bottom or base) for NO3 and as PDLb for DIP. This layer vertically extends between the MLD and the nitracline (phosphacline) depth (Fig. 2). The latter interface is estimated by the depth of NO3 (DIP) depletion, which is the deepest isopyenal at which micromolar NO3 (DIP) is zero (Kamykowski and Zentara, 1985; Omand and Mahadevan, 2015). The NO3 (DIP) depletion density is estimated at every discrete profile of micromolar NO3 (DIP) concentration by the intercept of the regression line reported in a nutrient-density diagram. There are various mechanisms, dynamical or biological, that can trigger exchanges of nutrients between the ML and NDLb (PDLb). Using the hypothesis of vertical (one- dimensional) regimes, there are two processes of exchange, by diffusion or advection (Du et al., 2017). The flux of nutrient can be expressed as: $F_{NO3} = F_{DIF} + F_{ADV}$ The diffusive flux F_{DIF} is expressed by the gradient of nutrient concentration times a vertical diffusivity coefficient K_x as: $F_{NO3} = F_{OIF} + K_{ADV}$ The diffusive flux F_{DIF} is expressed by the gradient of nutrient concentration times a vertical diffusivity coefficient K_x as discussed in Taillandier et al. (2020). The advective flux F_{ADV} corresponds either to the entrainment of deeper water in the mixed layer due to the erosion of the near-surface pycnocline, or to the detrainment of waters below the mixed layer by restratification, depending on the variations in wind stress and solar heating (Cullen et al., 2002). It is expressed as the variation in the nutrient concentration across the ML times the temporal variation of the MLD, as: $F_{ADV} = (NO3_{ML} - NO3_{NDLb}) x dMLD / dt$	mass content (i.e., the vertical integral of the density anomaly relative to surface) was equal to		Supprimé:
In the Mediterranean Sea, the low nutrient availability combined with a shallow mixed layer (ML) lead to the formation of a nutrient depleted layer that extend below the ML. Hereafter, the nutrient depleted layer is referred tq 'NDLb' (b for bottom or base) for NO3 and as PDLb (for DIP. This layer vertically extends between the MLD and the nitracline (phosphacline) depth (Fig. 2). The latter interface is estimated by the depth of NO3 (DIP) depletion, which is the deepest isopycnal at which micromolar NO3 (DIP) is zero (Kamykowski and Zentara, 1985; Omand and Mahadevan, 2015). The NO3 (DIP) depletion density is estimated at every discrete profile of micromolar NO3 (DIP) concentration by the intercept of the regression line reported in a nutrient-density diagram. There are various mechanisms, dynamical or biological, that can trigger exchanges of nutrients between the ML and NDLb (PDLb). Using the hypothesis of vertical (one- dimensional) regimes, there are two processes of exchange, by diffusion or advection (Du et al., 2017). The flux of nutrient can be expressed as: $F_{NO3} = F_{DIF} + F_{ADV}$ Superimé: the surface layers of the PEACETIME stations was assessed to be $10^5 \text{ m}^2 \text{ s}^{-1}$, as discussed in Taillandier et al. (2020). The advective flux F_{ADV} corresponds either to the entrainment of deeper water in the mixed layer due to the errosion of the near-surface pycnocline, or to the detrainment of waters below the mixed layer by restratification, depending on the variations in wind stress and solar heating (Cullen et al., 2002). It is expressed as the variation in the nutrient concentration across the ML times the temporal variation of the MLD, as: $F_{ADV} = (NO3_{NL} - NO3_{NDLb}) \times dMLD / dt$ Supprimé: taxSynallow ML is as the ones observed in this study (10 - 20 m) are primarily influenced by wind bursts that can lead to intermittent variations of the MLD, up	1 kg m ⁻² (Prieur et al., 2020), with an error of estimation of 0.5 m relative to the vertical		Supprimé: i
(ML) lead to the formation of a nutrient depleted layer that extend below the ML. Hereafter, the nutrient depleted layer is referred to 'NDLb' (b for bottom or base) for NO3 and as PDLb for DIP. This layer vertically extends between the MLD and the nitracline (phosphacline) depth (Fig. 2). The latter interface is estimated by the depth of NO3 (DIP) depletion, which is the deepest isopycnal at which micromolar NO3 (DIP) is zero (Kamykowski and Zentara, 1985; Omand and Mahadevan, 2015). The NO3 (DIP) depletion density is estimated at every discrete profile of micromolar NO3 (DIP) concentration by the intercept of the regression line 	resolution of the profile (1 m).		
the nutrient depleted layer is referred to 'NDLb' (b for bottom or base) for NO3 and as PDLb for DIP. This layer vertically extends between the MLD and the nitracline (phosphacline) depth (Fig. 2). The latter interface is estimated by the depth of NO3 (DIP) depletion, which is the deepest isopycnal at which micromolar NO3 (DIP) is zero (Kamykowski and Zentara, 1985; Omand and Mahadevan, 2015). The NO3 (DIP) depletion density is estimated at every discrete profile of micromolar NO3 (DIP) concentration by the intercept of the regression line reported in a nutrient-density diagram. There are various mechanisms, dynamical or biological, that can trigger exchanges of nutrients between the ML and NDLb (PDLb). Using the hypothesis of vertical (one- dimensional) regimes, there are two processes of exchange, by diffusion or advection (Du et al., 2017). The flux of nutrient can be expressed as: $F_{NO1} = F_{DIF} + F_{ADV}$ The diffusive flux F_{DIF} is expressed by the gradient of nutrient concentration times a vertical diffusivity coefficient K _x as: $F_{DIF} = K_x x (NO3_{ML} - NO3_{NDLb}) / MLD$ The typical magnitude of K _x in the surface layers of the PEACETIME stations was assessed to be $10^5 \text{ m}^2 \text{ s}^{-1}$, as discussed in Taillandier et al. (2020). The advective flux F_{ADV} corresponds either to the entrainment of deeper water in the mixed layer due to the erosion of the near-surface pycnocline, or to the detrainment of waters below the mixed layer by restratification, depending on the variations in wind stress and solar heating (Cullen et al., 2002). It is expressed as the variation in the nutrient concentration across the ML times the temporal variation of the MLD, as: $F_{ADV} = (NO3_{ML} - NO3_{NDLb}) x dMLD / dt$ Supprimé: sa Supprimé: sa Supprimé: sa Supprimé: bad sa' ¹) in the MLD. <u>Resulting</u> advective fluxes provide transient exchanges that are one order of s ²) in the MLD. <u>Resulting</u> advective fluxes provide transient exchanges that are one order of Supprimé	0 In the Mediterranean Sea, the low nutrient availability combined with a shallow mixed layer		Supprimé: the current case of
for DIP. This layer vertically extends between the MLD and the nitracline (phosphacline)Layer theoremdepth (Fig. 2). The latter interface is estimated by the depth of NO3 (DIP) depletion, which isSupprimé: hereafor asdepth (Fig. 2). The latter interface is estimated by the depth of NO3 (DIP) depletion, which isSupprimé: hereafor asis the deepest isopycnal at which micromolar NO3 (DIP) concentration by the intercept of the regression lineSupprimé: the cauting the1985; Omand and Mahadevan, 2015). The NO3 (DIP) depletion density is estimated at everySupprimé: the cauting thediscrete profile of micromolar NO3 (DIP) concentration by the intercept of the regression lineSupprimé: the cauting thereported in a nutrient-density diagram.There are various mechanisms, dynamical or biological, that can trigger exchanges ofnutrients between the ML and NDLb (PDLb). Using the hypothesis of vertical (one-Supprimé: the caution (Du etal., 2017). The flux of nutrient can be expressed as: $F_{NO1} = F_{DIF} + F_{ADV}$ The diffusive flux $F_{DIF} = K_x$ (NO3 _{ML} – NO3 _{NDLb}) / MLDThe typical magnitude of K_x in the surface layers of the PEACETIME stations was assessedto be $10^5 \text{ m}^2 \text{ s}^1$, as discussed in Taillandier et al. (2020).Supprimé: isthe advective flux F_{ADV} corresponds either to the entrainment of deeper water in the mixedlayer due to the encorsion of the near-surface pycnocline, or to the detrainment of waters belowthe mixed layer by restratification, depending on the variations in wind stress, and solarheating (Cullen et al., 2002). It is expressed as the variation in the nutrient concentrationacross the ML times the temporal variat	(ML) lead to the formation of a nutrient depleted layer that extend below the ML. Hereafter,		Supprimé: in such a LNLC system, the
for DJP. This layer vertically extends between the MLD and the nitracline (phosphacline)Supprime: hereafter asdepth (Fig. 2). The latter interface is estimated by the depth of NO3 (DIP) depletion, which isSupprime: when examining the5the deepest isopycnal at which micromolar NO3 (DIP) is zero (Kamykowski and Zentara, 1985; Omand and Mahadevan, 2015). The NO3 (DIP) depletion density is estimated at every discrete profile of micromolar NO3 (DIP) concentration by the intercept of the regression line reported in a nutrient-density diagram.Supprime: when examining the Supprime: when examining the Supprime: second at an utrient-density diagram.There are various mechanisms, dynamical or biological, that can trigger exchanges of 0 nutrients between the ML and NDLb (PDLb). Using the hypothesis of vertical (one- dimensional) regimes, there are two processes of exchange, by diffusion or advection (Du et al., 2017). The flux of nutrient can be expressed as: $F_{NO3} = F_{DIF} + F_{ADV}$ Supprime: second at an utrient can be expressed as: $F_{DiF} = K_x x (NO3_{ML} - NO3_{NDLb}) / MLD$ The diffusivity coefficient K _x as: $F_{DiF} = K_x x (NO3_{ML} - NO3_{NDLb}) / MLD$ Supprime: isThe typical magnitude of K _x in the surface layers of the PEACETIME stations was assessed to be 10 ⁵ m ² s ⁻¹ , as discussed in Taillandier et al. (2020). The advective flux F _{ADV} corresponds either to the entrainment of deeper water in the mixed layer due to the ensoin of the near-surface pycnocline, or to the detrainment of waters below the mixed layer by restratification, depending on the variations in wind stress, and solar heating (Cullen et al., 2002). It is expressed as the variation in the nutrient concentration across the ML times the temporal variation of the MLD, as: $F_{ADV} = (NO3_{ML} - NO3_{NDLb}) $	the nutrient depleted layer is referred to, 'NDLb' (b for bottom or base) for NO3 and as PDLb		
depth (Fig. 2). The latter interface is estimated by the depth of NO3 (DIP) depletion, which isisthe deepest isopycnal at which micromolar NO3 (DIP) is zero (Kamykowski and Zentara, 1985; Omand and Mahadevan, 2015). The NO3 (DIP) depletion density is estimated at every discrete profile of micromolar NO3 (DIP) concentration by the intercept of the regression line reported in a nutrient-density diagram. There are various mechanisms, dynamical or biological, that can trigger exchanges of nutrients between the ML and NDLb (PDLb). Using the hypothesis of vertical (one- dimensional) regimes, there are two processes of exchange, by diffusion or advection (Du et al., 2017). The flux of nutrient can be expressed as: $F_{NO1} = F_{DIF} + F_{ADV}$ The diffusive flux F_{DIF} is expressed by the gradient of nutrient concentration times a vertical if thisvive coefficient K _x as: $F_{DIF} = K_x \times (NO3_{ML} - NO3_{NDLb}) / MLD$ Supprimé: densityThe typical magnitude of K_z in the surface layers of the PEACETIME stations was assessed to be $10^5 \text{ m}^2 \text{ s}^{-1}$, as discussed in Taillandier et al. (2020). The advective flux F_{ADV} corresponds either to the entrainment of deeper water in the mixed layer due to the erosion of the near-surface pycnocline, or to the detrainment of waters below the mixed layer by restratification, depending on the variations in wind stress and solar heating (Cullen et al., 2002). It is expressed as the variation in the nutrient concentration across the ML times the temporal variation of the MLD, as: $F_{ADV} = (NO3_{ML} - NO3_{NDLb}) x dMLD / dt$ Supprimé: ta Supprimé: ta Supprimé: ta Supprimé: tal Supprimé: tal 	for DIP. This layer vertically extends between the MLD and the nitracline (phosphacline)	\bigcirc	
The deepest isopycnal at which micromolar NOS (DIP) is zero (Kamykowski and Zentara, 1985; Omand and Mahadevan, 2015). The NO3 (DIP) depletion density is estimated at every discrete profile of micromolar NO3 (DIP) concentration by the intercept of the regression line reported in a nutrient-density diagram. There are various mechanisms, dynamical or biological, that can trigger exchanges of nutrients between the ML and NDLb (PDLb). Using the hypothesis of vertical (one- dimensional) regimes, there are two processes of exchange, by diffusion or advection (Du et al., 2017). The flux of nutrient can be expressed as: $F_{NO3} = F_{DIF} + F_{ADV}$ The diffusivity coefficient K _z as: $F_{DIF} = K_z x (NO3_{NL-} - NO3_{NDLb}) / MLD$ The typical magnitude of K _z in the surface layers of the PEACETIME stations was assessed to be 10 ⁵ m ² s ⁻¹ , as discussed in Taillandier et al. (2020). The advective flux F _{ADV} corresponds either to the entrainment of deeper water in the mixed layer due to the errosion of the near-surface pycnocline, or to the detrainment of waters below the mixed layer by restratification, depending on the variations in wind stress and solar heating (Cullen et al., 2002). It is expressed as the variation in the nutrient concentration across the ML times the temporal variation of the MLD, as: $F_{ADV} = (NO3_{ML} - NO3_{NDLb}) x dMLD / dt$ Shallow MLs as the ones observed in this study (10 - 20 m) are primarily influenced by wind bursts that can lead to intermittent variations of the MLD, up to several meters per day (10 ⁵ m s ⁻¹) in the MLD. Resulting advective fluxes provide transient exchanges that are one order of	depth (Fig. 2). The latter interface is estimated by the depth of NO3 (DIP) depletion, which is	$\langle \rangle \rangle$	Supprimé: when examining the
Supprime: when considering the DP discrete profile of micromolar NO3 (DIP) concentration by the intercept of the regression line reported in a nutrient-density diagram.Supprime: when considering the DP discrete profile of micromolar NO3 (DIP) concentration by the intercept of the regression line reported in a nutrient-density diagram.There are various mechanisms, dynamical or biological, that can trigger exchanges of nutrients between the ML and NDLb (PDLb). Using the hypothesis of vertical (one- dimensional) regimes, there are two processes of exchange, by diffusion or advection (Du et al., 2017). The flux of nutrient can be expressed as: $F_{NO3} = F_{DIF} + F_{ADV}$ Supprime: the Supprime: tailThe diffusive flux Four is expressed by the gradient of nutrient concentration times a vertical diffusivity coefficient Kz as: $F_{DIF} = K_z x (NO3_{ML} - NO3_{NDLb}) / MLD$ Supprime: iThe typical magnitude of Kz in the surface layers of the PEACETIME stations was assessed to be 10 ⁵ m ² s ⁻¹ , as discussed in Taillandier et al. (2020). The advective flux FADV corresponds either to the entrainment of deeper water in the mixed layer due to the erosion of the near-surface pycnocline, or to the detrainment of waters below the mixed layer by restratification, depending on the variations in wind stress, and solar heating (Cullen et al., 2002). It is expressed as the variation in the nutrient concentration across the ML times the temporal variation of the MLD, as: $F_{ADV} = (NO3_{ML} - NO3_{NDLh}) x dMLD / dt$ Supprimé: taiShallow MLs as the ones observed in this study (10 - 20 m) are primarily influenced by wind bursts that can lead to intermittent variations of the MLD, up to several meters per day (10 ⁵ m s ⁻¹) in the MLD. Resulting advective fluxes provide transient exchanges that are one order ofSupprim		$\backslash /$	
discrete profile of micromolar NO3 (DIP) concentration by the intercept of the regression line reported in a nutrient-density diagram. There are various mechanisms, dynamical or biological, that can trigger exchanges of nutrients between the ML and NDLb (PDLb). Using the hypothesis of vertical (one- dimensional) regimes, there are two processes of exchange, by diffusion or advection (Du et al., 2017). The flux of nutrient can be expressed as: $F_{NO3} = F_{DIF} + F_{ADV}$ The diffusive flux F_{DIF} is expressed by the gradient of nutrient concentration times a vertical diffusivity coefficient K _z as: $F_{DIF} = K_z \times (NO3_{ML} - NO3_{NDLb}) / MLD$ The typical magnitude of K _z in the surface layers of the PEACETIME stations was assessed to be $10^5 \text{ m}^2 \text{ s}^{-1}$, as discussed in Taillandier et al. (2020). The advective flux F_{ADV} corresponds either to the entrainment of deeper water in the mixed layer due to the erosion of the near-surface pycnocline, or to the detrainment of waters below the mixed layer by restratification, depending on the variations in wind stress and solar heating (Cullen et al., 2002). It is expressed as the variation in the nutrient concentration across the ML times the temporal variation of the MLD, as: $F_{ADV} = (NO3_{NL-} - NO3_{NDLb}) \times dMLD / dt$ Shallow MLs as the ones observed in this study (10 - 20 m) are primarily influenced by wind bursts that can lead to intermittent variations of the MLD, up to several meters per day (10 ⁵ m s ⁻¹) in the MLD. Resulting advective fluxes provide transient exchanges that are one order of			
reported in a nutrient-density diagram. There are various mechanisms, dynamical or biological, that can trigger exchanges of nutrients between the ML and NDLb (PDLb). Using the hypothesis of vertical (one- dimensional) regimes, there are two processes of exchange, by diffusion or advection (Du et al., 2017). The flux of nutrient can be expressed as: $F_{NO3} = F_{DIF} + F_{ADV}$ The diffusive flux F_{DIF} is expressed by the gradient of nutrient concentration times a vertical diffusivity coefficient K _z as: $F_{DIF} = K_z \times (NO3_{ML} - NO3_{NDLb}) / MLD$ The typical magnitude of K _z in the surface layers of the PEACETIME stations was assessed to be $10^5 \text{ m}^2 \text{ s}^{-1}$, as discussed in Taillandier et al. (2020). The advective flux F_{ADV} corresponds either to the entrainment of deeper water in the mixed layer due to the erosion of the near-surface pycnocline, or to the detrainment of waters below the mixed layer by restratification, depending on the variations in wind stress and solar heating (Cullen et al., 2002). It is expressed as the variation in the nutrient concentration across the ML times the temporal variation of the MLD, as: $F_{ADV} = (NO3_{NL-} NO3_{NDLb}) \times dMLD / dt$ Supprimé: s . Supprimé: hat . Supp			Supprimé: the
There are various mechanisms, dynamical or biological, that can trigger exchanges of nutrients between the ML and NDLb (PDLb). Using the hypothesis of vertical (one- dimensional) regimes, there are two processes of exchange, by diffusion or advection (Du et al., 2017). The flux of nutrient can be expressed as: $F_{NO3} = F_{DIF} + F_{ADV}$ The diffusive flux F_{DIF} is expressed by the gradient of nutrient concentration times a vertical diffusivity coefficient K_z as: $F_{DIF} = K_z x (NO3_{ML} - NO3_{NDLb}) / MLD$ The typical magnitude of K_z in the surface layers of the PEACETIME stations was assessed to be $10^{-5} \text{ m}^2 \text{ s}^{-1}$, as discussed in Taillandier et al. (2020). The advective flux F_{ADV} corresponds either to the entrainment of deeper water in the mixed layer due to the erosion of the near-surface pycnocline, or to the detrainment of waters below the mixed layer by restratification, depending on the variations in wind stress and solar heating (Cullen et al., 2002). It is expressed as the variation in the nutrient concentration across the ML times the temporal variation of the MLD, as: $F_{ADV} = (NO3_{ML} - NO3_{NDLb}) x dMLD / dt$ Supprimé: as Supprimé: bat can lead to intermittent variations of the MLD, up to several meters per day (10^{-5} m s ⁻¹) in the MLD. <u>Resulting</u> advective fluxes provide transient exchanges that are one order of			Supprimé: density
nutrients between the ML and NDLb (PDLb). Using the hypothesis of vertical (one-dimensional) regimes, there are two processes of exchange, by diffusion or advection (Du et al., 2017). The flux of nutrient can be expressed as: $F_{NO3} = F_{DIF} + F_{ADV}$ The diffusive flux F_{DIF} is expressed by the gradient of nutrient concentration times a vertical diffusivity coefficient K_z as: $F_{DIF} = K_z x (NO3_{ML} - NO3_{NDLb}) / MLD$ The typical magnitude of K_z in the surface layers of the PEACETIME stations was assessed to be $10^{-5} \text{ m}^2 \text{ s}^{-1}$, as discussed in Taillandier et al. (2020). The advective flux F_{ADV} corresponds either to the entrainment of deeper water in the mixed layer due to the erosion of the near-surface pycnocline, or to the detrainment of waters below the mixed layer by restratification, depending on the variations in wind stress and solar heating (Cullen et al., 2002). It is expressed as the variation in the nutrient concentration across the ML times the temporal variation of the MLD, as: $F_{ADV} = (NO3_{ML} - NO3_{NDLb}) x dMLD / dt$ Shallow MLs as the ones observed in this study (10 - 20 m) are primarily influenced by wind bursts that can lead to intermittent variations of the MLD, up to several meters per day (10 ⁻⁵ m single supprimé: is is supprimé: is supprimé: is supprimé: is is			
dimensional) regimes, there are two processes of exchange, by diffusion or advection (Du et al., 2017). The flux of nutrient can be expressed as: $F_{NO3} = F_{DIF} + F_{ADV}$ The diffusive flux F_{DIF} is expressed by the gradient of nutrient concentration times a vertical diffusivity coefficient K_z as: $F_{DIF} = K_z \times (NO3_{ML} - NO3_{NDLb}) / MLD$ The typical magnitude of K_z in the surface layers of the PEACETIME stations was assessed to be $10^{-5} \text{ m}^2 \text{ s}^{-1}$, as discussed in Taillandier et al. (2020). The advective flux F_{ADV} corresponds either to the entrainment of deeper water in the mixed layer due to the erosion of the near-surface pycnocline, or to the detrainment of waters below the mixed layer by restratification, depending on the variations in wind stress and solar heating (Cullen et al., 2002). It is expressed as the variations in the nutrient concentration across the ML times the temporal variation of the MLD, as: $F_{ADV} = (NO3_{ML} - NO3_{NDLb}) \times dMLD / dt$ Shallow MLs as the ones observed in this study (10 - 20 m) are primarily influenced by wind bursts that can lead to intermittent variations of the MLD, up to several meters per day (10 ⁻⁵ m s ⁻¹) in the MLD. Resulting advective fluxes provide transient exchanges that are one order of			
al., 2017). The flux of nutrient can be expressed as: $F_{NO3} = F_{DIF} + F_{ADV}$ The diffusive flux F_{DIF} is expressed by the gradient of nutrient concentration times a vertical diffusivity coefficient K_z as: $F_{DIF} = K_z x (NO3_{ML} - NO3_{NDLb}) / MLD$ The typical magnitude of K_z in the surface layers of the PEACETIME stations was assessed to be 10^{-5} m ² s ⁻¹ , as discussed in Taillandier et al. (2020). The advective flux F_{ADV} corresponds either to the entrainment of deeper water in the mixed layer due to the erosion of the near-surface pycnocline, or to the detrainment of waters below the mixed layer by restratification, depending on the variations in wind stress and solar heating (Cullen et al., 2002). It is expressed as the variation in the nutrient concentration across the ML times the temporal variation of the MLD, as: $F_{ADV} = (NO3_{ML} - NO3_{NDLb}) x dMLD / dt$ Syhallow MLs as the ones observed in this study (10 - 20 m) are primarily influenced by wind bursts that can lead to intermittent variations of the MLD, up to several meters per day (10 ⁻⁵ m s ⁻¹) in the MLD. Resulting advective fluxes provide transient exchanges that are one order of Supprimé: that Supprimé: that			
$F_{DIF} + F_{ADV}$ The diffusive flux F_{DIF} is expressed by the gradient of nutrient concentration times a verticaldiffusivity coefficient K_z as: $F_{DIF} = K_z \ x (NO3_{ML} - NO3_{NDLb}) / MLD$ The typical magnitude of K_z in the surface layers of the PEACETIME stations was assessedto be $10^{-5} m^2 s^{-1}$, as discussed in Taillandier et al. (2020).The advective flux F_{ADV} corresponds either to the entrainment of deeper water in the mixedlayer due to the erosion of the near-surface pycnocline, or to the detrainment of waters belowthe mixed layer by restratification, depending on the variations in wind stress and solarheating (Cullen et al., 2002). It is expressed as the variation in the nutrient concentrationacross the ML times the temporal variation of the MLD, as: $F_{ADV} = (NO3_{ML} - NO3_{NDLb}) x dMLD / dt$ Supprimé: $A = S$ <td>dimensional) regimes, there are two processes of exchange, by diffusion or advection (Du et</td> <td></td> <td></td>	dimensional) regimes, there are two processes of exchange, by diffusion or advection (Du et		
The diffusive flux F_{DIF} is expressed by the gradient of nutrient concentration times a vertical diffusivity coefficient K_z as: $F_{DIF} = K_z x (NO3_{ML} - NO3_{NDLb}) / MLD$ The typical magnitude of K_z in the surface layers of the PEACETIME stations was assessed to be $10^{-5} m^2 s^{-1}$, as discussed in Taillandier et al. (2020). The advective flux F_{ADV} corresponds either to the entrainment of deeper water in the mixed layer due to the erosion of the near-surface pycnocline, or to the detrainment of waters below the mixed layer by restratification, depending on the variations in wind stress and solar heating (Cullen et al., 2002). It is expressed as the variation in the nutrient concentration across the ML times the temporal variation of the MLD, as: $F_{ADV} = (NO3_{ML} - NO3_{NDLb}) x dMLD / dt$ Symptimé: $A = S$ Supprimé: $A = S$	al., 2017). The flux of nutrient can be expressed as:		
diffusivity coefficient Kz as: $F_{DIF} = K_z x (NO3_{ML} - NO3_{NDLb}) / MLD$ The typical magnitude of Kz in the surface layers of the PEACETIME stations was assessed Supprimé: i to be 10 ⁻⁵ m ² s ⁻¹ , as discussed in Taillandier et al. (2020). Supprimé: i The advective flux FADV corresponds either to the entrainment of deeper water in the mixed Iayer due to the erosion of the near-surface pycnocline, or to the detrainment of waters below the mixed layer by restratification, depending on the variations in wind stress, and solar Supprimé: es heating (Cullen et al., 2002). It is expressed as the variation in the nutrient concentration across the ML times the temporal variation of the MLD, as: Supprimé: near Supprimé: es FADV = (NO3_{ML} - NO3_{NDLb}) x dMLD / dt Supprimé: As Susts that can lead to intermittent variations of the MLD, up to several meters per day (10 ⁻⁵ m s ⁻¹) in the MLD. Resulting advective fluxes provide transient exchanges that are one order of Supprimé: hat	$F_{\rm NO3} = F_{\rm DIF} + F_{\rm ADV}$		
$F_{DIF} = K_z x (NO3_{ML} - NO3_{NDLb}) / MLD$ The typical magnitude of K_z in the surface layers of the PEACETIME stations was assessedto be $10^{-5} m^2 s^{-1}$, as discussed in Taillandier et al. (2020).The advective flux F_{ADV} corresponds either to the entrainment of deeper water in the mixedlayer due to the erosion of the near-surface pycnocline, or to the detrainment of waters belowthe mixed layer by restratification, depending on the variations in wind stress and solarheating (Cullen et al., 2002). It is expressed as the variation in the nutrient concentrationacross the ML times the temporal variation of the MLD, as: $F_{ADV} = (NO3_{ML} - NO3_{NDLb}) x dMLD / dt$ Shallow MLs as the ones observed in this study (10 - 20 m) are primarily influenced by windbursts that can lead to intermittent variations of the MLD, up to several meters per day (10 ⁻⁵ ms ⁻¹) in the MLD. Resulting advective fluxes provide transient exchanges that are one order of	The diffusive flux F_{DIF} is expressed by the gradient of nutrient concentration times a vertical		
The typical magnitude of K_z in the surface layers of the PEACETIME stations was assessedSupprimé: ito be $10^{-5} m^2 s^{-1}$, as discussed in Taillandier et al. (2020).The advective flux F_{ADV} corresponds either to the entrainment of deeper water in the mixed10layer due to the erosion of the near-surface pycnocline, or to the detrainment of waters belowthe mixed layer by restratification, depending on the variations in wind stress, and solarheating (Cullen et al., 2002). It is expressed as the variation in the nutrient concentrationacross the ML times the temporal variation of the MLD, as: $F_{ADV} = (NO3_{ML} - NO3_{NDLb}) x dMLD / dt$ Shallow MLs as the ones observed in this study (10 - 20 m) are primarily influenced by windbursts that can lead to intermittent variations of the MLD, up to several meters per day (10 ⁻⁵ ms^{-1}) in the MLD. Resulting advective fluxes provide transient exchanges that are one order of	diffusivity coefficient K _z as:		
to be 10^{-5} m ² s ⁻¹ , as discussed in Taillandier et al. (2020). The advective flux F_{ADV} corresponds either to the entrainment of deeper water in the mixed layer due to the erosion of the near-surface pycnocline, or to the detrainment of waters below the mixed layer by restratification, depending on the variations in wind stress, and solar heating (Cullen et al., 2002). It is expressed as the variation in the nutrient concentration across the ML times the temporal variation of the MLD, as: $F_{ADV} = (NO3_{ML} - NO3_{NDLb}) x dMLD / dt$ Shallow MLs as the ones observed in this study (10 - 20 m) are primarily influenced by wind bursts that can lead to intermittent variations of the MLD, up to several meters per day (10^{-5} m s ⁻¹) in the MLD. Resulting advective fluxes provide transient exchanges that are one order of	$F_{DIF} = K_z x (NO3_{ML} - NO3_{NDLb}) / MLD$		
The advective flux F_{ADV} corresponds either to the entrainment of deeper water in the mixed layer due to the erosion of the near-surface pycnocline, or to the detrainment of waters below the mixed layer by restratification, depending on the variations in wind stress and solar heating (Cullen et al., 2002). It is expressed as the variation in the nutrient concentration across the ML times the temporal variation of the MLD, as: $F_{ADV} = (NO3_{ML} - NO3_{NDLb}) x dMLD / dt$ Shallow MLs as the ones observed in this study (10 - 20 m) are primarily influenced by wind bursts that can lead to intermittent variations of the MLD, up to several meters per day (10 ⁻⁵ m s ⁻¹) in the MLD. Resulting advective fluxes provide transient exchanges that are one order of	The typical magnitude of K_z in the surface layers of the PEACETIME stations was assessed		Supprimé: i
layer due to the erosion of the near-surface pycnocline, or to the detrainment of waters below the mixed layer by restratification, depending on the variations in wind stress and solarSupprimé: esheating (Cullen et al., 2002). It is expressed as the variation in the nutrient concentration across the ML times the temporal variation of the MLD, as: $F_{ADV} = (NO3_{ML} - NO3_{NDLb}) \times dMLD / dt$ Supprimé: esShallow MLs as the ones observed in this study (10 - 20 m) are primarily influenced by wind bursts that can lead to intermittent variations of the MLD, up to several meters per day (10 ⁻⁵ m s ⁻¹) in the MLD. Resulting advective fluxes provide transient exchanges that are one order ofSupprimé: that Supprimé: These	to be 10^{-5} m ² s ⁻¹ , as discussed in Taillandier et al. (2020).		
the mixed layer by restratification, depending on the variations in wind stress and solar heating (Cullen et al., 2002). It is expressed as the variation in the nutrient concentration across the ML times the temporal variation of the MLD, as: $F_{ADV} = (NO3_{ML} - NO3_{NDLb}) \times dMLD / dt$ Shallow MLs as the ones observed in this study (10 - 20 m) are primarily influenced by wind bursts that can lead to intermittent variations of the MLD, up to several meters per day (10 ⁻⁵ m s ⁻¹) in the MLD. Resulting advective fluxes provide transient exchanges that are one order of	The advective flux F_{ADV} corresponds either to the entrainment of deeper water in the mixed		
heating (Cullen et al., 2002). It is expressed as the variation in the nutrient concentration across the ML times the temporal variation of the MLD, as: $F_{ADV} = (NO3_{ML} - NO3_{NDLb}) \times dMLD / dt$ Supprimé: A sShallow MLs as the ones observed in this study (10 - 20 m) are primarily influenced by wind bursts that can lead to intermittent variations of the MLD, up to several meters per day (10 ⁻⁵ m s ⁻¹) in the MLD. Resulting advective fluxes provide transient exchanges that are one order ofSupprimé: A s Supprimé: is Supprimé: that Supprimé: These	layer due to the erosion of the near-surface pycnocline, or to the detrainment of waters below		
across the ML times the temporal variation of the MLD, as: $F_{ADV} = (NO3_{ML} - NO3_{NDLb}) \times dMLD / dt$ Shallow MLs as the ones observed in this study (10 - 20 m) are primarily influenced by windbursts that can lead to intermittent variations of the MLD, up to several meters per day (10 ⁻⁵ ms ⁻¹) in the MLD. Resulting advective fluxes provide transient exchanges that are one order ofSupprimé: These	the mixed layer by restratification, depending on the variations in wind stress, and solar		Supprimé: es
$F_{ADV} = (NO3_{ML} - NO3_{NDLb}) \times dMLD / dt$ Schallow MLs as the ones observed in this study (10 - 20 m) are primarily influenced by wind bursts that can lead to intermittent variations of the MLD, up to several meters per day (10 ⁻⁵ m s ⁻¹) in the MLD. Resulting advective fluxes provide transient exchanges that are one order of Supprimé: These	heating (Cullen et al., 2002). It is expressed as the variation in the nutrient concentration		
Shallow MLs as the ones observed in this study (10 - 20 m) are primarily influenced by wind Supprimé: A s bursts that can lead to intermittent variations of the MLD, up to several meters per day (10 ⁻⁵ m Supprimé: is s ⁻¹) in the MLD. Resulting advective fluxes provide transient exchanges that are one order of Supprimé: that	across the ML times the temporal variation of the MLD, as:		
bursts <u>that can</u> lead to intermittent variations of <u>the MLD, up to</u> several meters per day (10 ⁻⁵ m s ⁻¹) in the MLD. <u>Resulting</u> advective fluxes provide transient exchanges that are one order of Supprimé : that Supprimé : that Supprimé : These	$F_{ADV} = (NO3_{ML} - NO3_{NDLb}) \times dMLD / dt$		
s ⁻¹) in the MLD. <u>Resulting</u> advective fluxes provide transient exchanges that are one order of Supprimé : that Supprimé : that	5 Shallow MLs as the ones observed in this study (10 - 20 m) are primarily influenced by wind		Supprimé: A s
s ⁻¹) in the MLD. <u>Resulting</u> advective fluxes provide transient exchanges that are one order of Supprimé: that Supprimé: These	bursts <u>that can</u> lead to intermittent variations of the MLD, up to several meters per day (10^{-5} m)		
			Supprime: These

scale of a significant atmospheric deposition, associated rapid variations of the MLD would

Supprimé: and the

- 580 rather promote, the input of atmospheric nutrients to be exported below the ML by advection rather than by diffusion. In other terms, using the hypothesis of non-stationary regimes due to rapid changes in atmospheric conditions (that control both the mixing state of the <u>ML</u> and atmospheric nutrient inputs), we assume that vertical advection is the main process of exchange.
- 585 At the short stations and sites, the term $NO3_{ML} NO3_{NDLb}$ can be inferred by the difference between mean nanomolar (LWCC) concentrations <u>within the NDLb and the ML_At short</u> stations, as advective fluxes could not be characterized, only a qualitative assessment of nutrient fluxes across ML is given. When $NO3_{ML} - NO3_{NDLb} < 0$, the NDLb is supplied with
- <u>NO3</u> across the nutricline, and could be then possibly transferred into the ML. This means
 that nutrients within the ML are impacted by inputs from below. When NO3_{ML}- NO3_{NDLb} > 0,
 the ML is supplied in <u>NO3</u> from the atmosphere which <u>is</u> further exported into the NDLb.
 Vertical distributions of DIP, along the longitudinal transect, are described in detail in a
 - companion paper (Pulido-Villena et al., 2021),

595 **2.4 Budget from the metabolic fluxes**

600

Trapezoidal integration was used to integrate BP, PP and N2fix within the ML. The biological activity at the surface was considered to be equal to that of the first layer sampled (around 5 m depth at the short stations, 1 m depth at the FAST site). When the MLD was not sampled, the volumetric activity at <u>that</u> depth was linearly interpolated between the 2 closest data points above and below the MLD.

We used an approach similar to Hoppe et al. (1993) to compute the *in situ* hydrolysis rates for LAP and AP. We assumed that total amino acids (TAA) could be representative of dissolved proteins. *In situ* hydrolysis rates of LAP and AP were determined using molar concentrations of TAA and L-DOP, respectively and used as the substrate concentration in the Michaelis-

- 605 Menten kinetics. For LAP, the transformation of *in situ* rates expressed in nmol TAA hydrolyzed L⁻¹ h⁻¹ were then transformed into nitrogen units using N per mole TAA, as the molar distributions of TAA were available. Integrated *in situ* LAP hydrolysis rates were calculated assuming the Michaelis-Menten parameters Vm and Km obtained at a 5 m depth to be representative of the whole ML. Thus an average *in situ* volumetric LAP flux in the ML
- 610 was obtained by combining the average TAA concentrations in the ML with these kinetic parameters, and multiplying this volumetric rate by the MLD. Daily BP, AP and LAP integrated activities were calculated from hourly rates x 24. Assuming no direct excretion of

Supprimé: , Supprimé: would preferentially be

Supprimé: interface

Supprimé: inside

Supprimé: the mean inside Supprimé: Since advective flux estimates require knowledge of the evolution of the MLD over time, such fluxes are only accessible at the sites. Supprimé: nutrients

Supprimé: nutrients Supprimé: are

Supprimé: In this study, we will focus on phosphate exchanges between the ML and PDLb and relationships with NO3 distribution only at the high-frequency sampled FAST site

Supprimé: this

either nitrogen or phosphorus, the quota C/N and C/P of cell demand is equivalent to the cell biomass quotas. We used molar C/N ratios derived from Moreno and Martiny (2018) (range 6-8, mean 7) for phytoplankton and from Nagata et al. (1986) for heterotrophic prokaryotes (range 6.2-8.4, mean 7.3). C/P of sorted cells (cyanobacteria, picophytoeukaryotes) in P depleted conditions ranged from 107 to 161 (Martiny et al., 2013), and we considered a mean

of 130 for phytoplankton. A value of 100 was used for heterotrophic prokaryotes (Godwin

635

640

and Cotner, 2015).

3. Results

3.1 Nutrient patterns and biological fluxes along the PEACETIME transect

The MLD ranged between 7 m at ST9 and 21 m at ST1 (Table S1, Fig. 3). The nitracline was shallow in the Provençal Basin (50 – 60 m), dropping to 70 m in the Eastern Algerian and Tyrrhenian Seas; becoming deeper in the Western Algerian and Ionian Seas (80 - 90 m, Table S1). Mean NO3 concentrations in the NDLb ranged from the quantification limit (9 nM) to 116 nM (Table S1, Fig. 4). In the ML, mean NO3 concentrations ranged from 9 to 135 nM.
For the 'group 1' stations (see Table S1), NO3 concentrations were low (below 50 nM) both within the ML and the NDLb, with weak gradient between the two layers. For the 'group 2' stations, NO3 concentrations were moderate (50 - 80 nM) both within the ML and the NDLb
but still exhibiting a small difference between the two layers, indicating again no significant instantaneous exchanges. For 'group 3', higher NO3 concentrations were measured in both the ML and the NDLb (> 80 nM) but the small positive differences (< 20 nM) between the two layers still indicate weak or negligible exchanges between the two layers. For 'group 4, high and moderate NO3 concentrations were measured within the ML and NDLb,

respectively, with a large positive difference (> 20 nM) between the layers. This indicates the presence of a gradient from the ML to the NDLb.

At 5 m depth, <u>the leucine aminopeptidase (LAP) kinetic parameter Vm ranged from 0.21 to</u> 0.56 nmol MCA-leu hydrolyzed I^{-1} h⁻¹, and Km LAP ranged from 0.12 to 1.29 μ M. The mean TAA within the ML ranged from 0.17 to 0.28 μ M. The mean *in situ* LAP hydrolysis rate

- 660
- within the ML, derived from these 3 series of parameters, ranged from 0.07 to 0.29 nmol N I^{-1} h⁻¹ (results not shown but detailed in Van Wambeke et al., 2021).

The vertical distributions of PP and BP for the short stations are described in Marañon et al. (2021). Briefly, PP exhibited a deep maximum close to the DCM depth or slightly above

Supprimé: the Supprimé: both Supprimé: differences precluding any

Supprimé: LAP

Supprimé: From these 3 series of parameters, we derived t Supprimé: which

680

whereas vertical distribution of BP generally showed 2 maxima, one within the mixed layer, and a second close to the DCM. Integrated PP (Table 1, Table S2) ranged from 138 (TYR17 May) to 284 (SD1) mg C m⁻² d⁻¹. Integrated BP (0-200 m) ranged from 44 (JON27May) to 113 (FAST+0.53) mg C m⁻² d⁻¹. Overall, at the time of the PEACETIME cruise, the transect exhibited the classical west-east gradient of increasing oligotrophy detected by ocean colour (see Fig. 8 in Guieu et al., 2020),

3.2 N budgets and fluxes at short stations

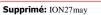
Biological rates (all expressed in N units) within the ML at the short stations were compared. (Table 2). Phytoplankton N demand (phytoN demand) was the greatest rate, followed by

- heterotrophic prokaryotic N demand (hprokN demand). On average, phytoN demand was 2.9 (range 1.5 – 8.1) times greater than that of hprokN, LAP hydrolysis rates represented between 14 and 66 % of the hprokN demand (mean \pm sd : 37% \pm 19%), N₂ fixation rates represented between 1 to 4.5% of the phytoN demand (2.6% \pm 1.3%) and 3 to 11% of the hprok N
- demand (6.4% \pm 2.4%). N₂ fixation rates integrated over the ML correlated slightly better with hprokN demand (r = 0.75) than with phytoN demand (r = 0.66).
 - Dissolved inorganic N (DIN=NO3+NH4) solubilized from dry atmospheric deposition ranged from 17 to 40 μ mol N m⁻² d⁻¹ <u>of which 79%</u> on average <u>were</u> NO3 (Table 2). This new DIN input was similar or higher than N₂ fixation rates within the ML (from 1.3 to 11 <u>fold</u>, mean, 4.8-fold). On average the new DIN from dry deposition represented 27% of the hprokN demand (range 10-82%) and 11% of the phytoN demand (range 1-30%) within the ML.

690

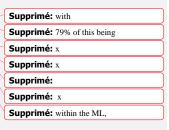
3.3 Biogeochemical evolution at the ION site

- The ION site was occupied May 25 to 29. Rain events in the vicinity of the ship were observed on May 26 and May 29 (Desboeufs et al., this issue, in prep). On the May 29 the rain event was associated with a rain front covering more than 5 000 km². A rain sample could be taken on board between 5:08 and 6:00 (local time), i.e. just 3 hours before the last CTD cast. The chemical composition of the rain indicated an anthropogenic background influence (Desboeufs et al., this issue, in prep.).
 - TDP solubilized from dry atmospheric deposition decreased from 268 nmol P m⁻² d⁻¹ May 25, -26 to 124 nmol P m⁻² d⁻¹ May 27, 28). DIN fluxes from dry atmospheric deposition averaged 29 \pm 4 µmol N m⁻² d⁻¹ with small variability during the occupation of the site (Table S2). The



Supprimé: in absence of a rain event the Mediterranean Sea,

Supprimé: , but with a large variability (min x1.5, max x8.1)



Supprimé: from the
Supprimé: 25th to the 29 th of
Supprimé: th
Supprimé: th
Supprimé: 29 th of

Supprimé: th
Supprimé: th
Supprimé: th
Supprimé: th
Supprimé: were on
Supprimé: no significant difference
Supprimé: In the rain, t

molar ratio DIN/DIP <u>in the rain</u> was 208 <u>and DOP represented</u> 60%, of the total dissolved P (Table 3).

730	CTD casts, dedicated to biogeochemical studies, were taken each 24 h for biological fluxes or
	48 h for DIP and NO3. Thus the time sequence for nutrients in the water column at ION is
	given for only by three profiles. The first profile (May 25 before rain events in the area) is
	'flat', corresponding to smooth weather conditions and a shallow ML with low and
	homogeneous concentrations of NO3 in the ML and the NDLb (Fig. 4). Shortly after, there
735	was an atmospheric depression: some rain events were observed in the area on May 26, but not
	on board and the ML started to deepen 13 h before the second cast with nutrient sampling (on
	May 27). This cast reflected high NO3 in the ML (Fig. 3). The mixing should have set up a
ļ	homogeneous ML, but wind conditions rose to 20 kt just at the time of the cast (Fig. 3). The
	interval between the second and the third cast sampling nutrients (May 29, cast done 3 hours
740	after the rain sampled on board) was marked by a slight relaxation of weather depression, and
	a deepening of the ML down to 20 m. This cast <u>reflected a NO3 decrease in both the ML and</u>
	NDLb, but with NO3 concentrations, higher in ML. The calculation of vertical advective
	fluxes between the two layers showed a downward flux in the first interval May 25-27 (Fig. 4,
	Table S1) and an upward flux in the second interval (May 27-29).
745	Due to the lack of high frequency sampling, it was also particularly difficult to assess the
	direct time evolution effects of dry atmospheric deposition at the ION site. Nevertheless, it
	was clear from the casts sampled on the May_27 and 29 , that this site was characteristic of
	group 4 (i.e. higher NO3 concentrations in the ML than in the NDLb), suggesting recent
	inputs from the atmosphere. Ectoenzymatic activities were only sampled on May 25. Vm of
750	LAP at 5 m (0.22 nmol N I^{-1} h^{-1}) was one of the lowest values recorded during the cruise
	whilst Vm of AP was the highest (5.6 nmol P $l^{-1} h^{-1}$). PP integrated over the euphotic zone
I	increased slightly from 188 to 226 mg C m ⁻² d ⁻¹ (Table S2), but due to changes in the MLD at
	the ION site (range 11-21 m) this trend was not visible when integrating PP over the ML.
	Integrated over the ML, BP increased slightly, from 7.5 to 10.3 mg C m ⁻² d ⁻¹ between May 25
755	and May 29, and indicated that hprok benefited more from the atmospheric inputs than the
I	autotrophs as PP decreased at 5m depth (Fig. S1, Table S2). The profiles of hprok and
	Synechococcus abundances showed no particular trend with time, with higher variations
	within the DCM (Fig. S1).

Supprimé: . Supprimé: in the collected rain was also an important Supprimé: source Supprimé: (Supprimé:) Supprimé: from that wet deposition Supprimé: 25th of Supprimé: fair

Supprimé: of rain
Supprimé: th
Supprimé: ,
Supprimé: sampling
Supprimé: s
Supprimé: the 27 th of
Supprimé: was marked by
Supprimé: nitrate
Supprimé: 29 th of
Supprimé: i
Supprimé: was marked by
Supprimé: values
Supprimé: were
Supprimé: Given the remaining signature at 15 m and the deepening of the ML, the two layers might have stayed isolated. However,
at 15 m and the deepening of the ML, the two layers might have stayed isolated.
at 15 m and the deepening of the ML, the two layers might have stayed isolated. However,
at 15 m and the deepening of the ML, the two layers might have stayed isolated. However, Supprimé: t
at 15 m and the deepening of the ML, the two layers might have stayed isolated. However, Supprimé: t Supprimé: May
at 15 m and the deepening of the ML, the two layers might have stayed isolated. However, Supprimé: t Supprimé: May Supprimé: May
at 15 m and the deepening of the ML, the two layers might have stayed isolated. However, Supprimé: t Supprimé: May Supprimé: May Supprimé: th
at 15 m and the deepening of the ML, the two layers might have stayed isolated. However, Supprimé: t Supprimé: May Supprimé: May Supprimé: th Supprimé: th
at 15 m and the deepening of the ML, the two layers might have stayed isolated. However, Supprimé: t Supprimé: May Supprimé: May Supprimé: th Supprimé: th Supprimé: th of May Supprimé: indicating
at 15 m and the deepening of the ML, the two layers might have stayed isolated. However, Supprimé: t Supprimé: May Supprimé: May Supprimé: th Supprimé: th of May Supprimé: indicating Supprimé: the
at 15 m and the deepening of the ML, the two layers might have stayed isolated. However, Supprimé: t Supprimé: May Supprimé: May Supprimé: th Supprimé: th Supprimé: indicating Supprimé: the Supprimé: to

760 3.4 N budgets and fluxes at the FAST site

During the <u>occupation of</u> the FAST site, two <u>rains episodes took place</u>: the evening of June 2-<u>night of June</u> 3, and the early morning of <u>June 5</u> (Tovar-Sanchez et al., 2020). <u>The rain radar</u> data indicated the presence of a rain front with patchy, numerous and intense rain events occurring over a large area surrounding the ship's location. These two episodes <u>coincided</u> with a dust plume transported in altitude (between 1 and 4 km) and resulted in wet deposition of dust (Desboeufs et al., this issue, in prep.). <u>A</u> rain <u>sample was collected</u> on board on June 5th (between 02:36 and 03:04, local time) and was associated with a dust wet deposition flux ~ 40 mg m⁻². The DIN/DIP ratio in the rain reached 480 (Table 3). After the rain, daily fluxes of DIN solubilized from dry aerosol deposition strongly decreased from 45 to 9.8 µmol N m⁻² d⁻¹ between June 4, and 5,

800

805

830

The beginning of the <u>water column</u> sampling at FAST site (-2.3; -1.5; -0.25) was marked by moderate and similar decreases in NO3 concentration within the ML and NDLb. Integrated stocks of NO3 within the ML (Table S2) reflected slight changes <u>of MLD</u> (from 14 to 10 m during this time interval). On June 5th, the rain event (Table 3) was associated with a strong wind burst and an abrupt mixing. The comparison between NO3 concentrations from two casts, sampled 6 h before and 6 h after the rain, (FAST-0.25 and FAST+0.24), showed a clear

- 815 N enrichment of the ML as mean NO3 increased from 56 to 93 nM and NO3 integrated stocks increased by 888 µmol N m⁻² (Fig. 3, Table S2). There was also clear difference in the mean NO3 concentrations between ML and NDLb (93 ± 15 vs 51 ± 7 nM, respectively). This is the highest NO3 difference observed during the cruise between these 2 layers (Fig. 4), confirming that this ML enrichment could not be attributed to inputs from below. The relaxation of this
- 820 wind burst was progressive, with a continuous deepening of the ML (Table S1). The export of the atmospheric NO3 into the NDLb was maximal after the rain event (FAST+0.24). At the end of the site occupation period (FAST+3.8) high NO3 concentrations (mean 135 nM) were measured again within the ML.

DIP concentration dynamics were different from those of NO3, with similar DIP integrated
 stocks within the ML being measured 6 h before and 6 h after the rain (136 µmol m⁻²). From then on, DIP stocks progressively increased reaching a maximum (281 µmol P m⁻²) one day after the rain (FAST+1).

Immediately after the rain, integrated PP (euphotic zone) decreased from 274 mg C m⁻² d⁻¹ (FAST-0.9) to 164 mg C m⁻² d⁻¹ (FAST+0.07) and continued to decrease the following day. It was only 3.8 days after the rain that the initial values (before the rain) of integrated PP could

Supprimé: time
Supprimé: at
Supprimé: periods of rains occurred
Supprimé: 2nd
Supprimé: rd
Supprimé: the 5th
Supprimé: On a spatial scale, t
Supprimé: were concomitant
Supprimé: The second
Supprimé: event was sampled

Supprimé: th	
Supprimé: th	

Supprimé: with
Supprimé: ¶

Supprimé: the
Supprimé: fluxes
Supprimé: similar
Supprimé: It is only f
Supprimé: that
Supprimé: flux

Supprimé: i

be observed again (Table S2). Such variations were mostly due to changes in volumetric rates within the DCM depth (Fig. S2), as the activity did not change significantly within the ML (28-33 mg C m⁻² d⁻¹, Fig. S2, Fig. 5). Integrated BP over 0-200 m showed the opposite trend to that of PP and tended to increase after the rain (from $86 \pm 3 \text{ mg C m}^{-2} \text{ d}^{-1}$ (n = 4) before, and 855 up to 113 mg C m⁻² d⁻¹ (FAST+0.5) after (Table S2)). Although modest, this increasing trend was also visible when integrating BP only over the ML (12-15 before; 15-19 mg C m⁻² d⁻¹ after). The abundances of picophytoplankton groups were mostly varying in the vicinity of the DCM depth with peaks occurring 1-2 days after the rain (grey profiles, Fig S3), in particular 860 for prokaryotes (Prochlorococcus, Synechococcus). Heterotrophic prokaryotes and nanoflagellate abundances slightly increased within the DCM depth after the rain.

4. Discussion

- 865 The specific context of the oceanographic survey constrained the temporal and spatial coverage of our analysis, as the biogeochemical responses to a rain event were investigated over a few days (3 - 5), and tens of km (40 - 50). Their evolution was restricted to the vertical dimension, integrating lateral exchanges by horizontal diffusion or local advection that occurred over the prescribed space and time scales. In the vertical dimension, exchanges of 870 nutrients across the ML were controlled by advection due to rapidly changing conditions (MLD fluctuations along with nutrient inputs from the atmosphere) rather than to diffusion
- between stationary pools. Four groups of stations, corresponding to different stages of ML enrichment and relaxation, due to the nutrient inputs from single rain events, have been characterized based on the differences in NO3 concentration between ML and NDLb (see
- 875 section 2.4). As shown in Fig. 4, this succession of stages is in agreement with the NO3 fluxes from above and below the ML. Moreover, they provide a temporal scaling of the oceanic response to atmospheric deposition, with a quasi-instantaneous change at the time of the rain event and a 2-day relaxation period to recover to pre-event conditions In this context, we will i) discuss the nitrogen budget within the ML at the short stations
- 880 considered as a 'snapshot', and ii) analyze in detail, using a time series of CTD casts, the biogeochemical changes within the ML and the NDLb following the atmospheric wet deposition event at the FAST site, discussing the possible modes of transfer of nutrients between these 2 layers.

-{	Supprimé: data
\neg	Supprimé: :
$\langle \rangle$	Supprimé: have been scaled
)	Supprimé: in time
	Supprimé: in space spanning

890	4.1 A snapshot of biological fluxes in the ML and their link to new DIN from		
	atmospheric dry deposition		
	The dependence of hprok on nutrients rather than on labile organic carbon during		
	stratification conditions is not uncommon in the MS (Van Wambeke et al., 2002, Céa et al,		
	2017; Sala et al., 2002) and has also been shown during PEACETIME cruise (P, or N,P		
895	colimitation, Fig. S4). Hprok have an advantage due to their small cell size and their kinetic		
	systems which are adapted to <u>extremely</u> low concentrations of nutrients (for example for DIP		Supprimé: ranges
I	see Talarmin et al., 2015). Under such conditions of limitation, hprok will react rapidly to		
	new phosphorus and nitrogen inputs, coming from atmospheric deposition. During an		
	artificial in situ DIP enrichment experiment in the Eastern Mediterranean, P rapidly circulated		
900	through hprok and heterotrophic ciliates, while the phytoplankton was not directly linked to		
	this 'bypass' process (Thingstad et al., 2005). Bioassays conducted in the tropical Atlantic		
	Ocean have also shown that hprok respond more strongly than phytoplankton to nutrients		
	from Saharan aerosols (Marañón et al. 2010), a pattern that has been confirmed in a meta-		
	analysis of dust addition experiments (Guieu et al., 2014; Guieu and Ridame, in press; Gazeau		Supprimé: in vitro
905	et al., 2021).		
	We considered hprokN demand together with phytoN demand and compared it to		
	autochthonous (DON hydrolysis by ectoenzymatic activity) and allochthonous (atmospheric		Supprimé: breakdown
I	deposition) sources. To the best of our knowledge this is the first time that these fluxes are		
910	compared based on their simultaneous guantification at sea. A high variability was observed		Supprimé: measurements
	among the 10 short stations (Table 2). The regeneration of nitrogen through aminopeptidase		Supprimé: between
I	activity was clearly the primary provider of N to hprok as 14 to 66% (mean \pmsd : 37% \pm		
	19%) of the hprokN demand could be satisfied by in situ LAP activity. Such percentages may		
	be largely biased by the conversion factors from C to N and propagation of errors for the LAP $% \mathcal{A}$		
915	hydrolysis rates and BP rates. However, the C/N ratio of hprok is relatively narrow under		
	large variations of P or N limitation (6.2 to 8.4; Nagata, 1986).		
	Other regeneration sources exist such as direct excretion of NH4 or low molecular weight		
	DON sources with no necessity for hydrolysis prior to uptake (Jumars et al., 1989). For		
	instance, Feliú et al. (2020) calculated that NH4 and DIP excretion by zooplankton would		
920	satisfy 25-43% of the phytoN demand and 22-37% of the phytoP demand over the whole		
	euphotic zone. Such percentages suggest that direct excretion by zooplankton along with		
	ectoenzymatic activity, provide substantial N for biological activity.	_	Supprimé: ,

N₂ fixation is also a source of new N that can directly fuel hprok as some diazotrophs are

- 930 heterotrophic (Delmont et al. 2018, and references therein), or indirectly, as part of the fixed N₂ that rapidly cycles through hprok (Caffin et al., 2018). Furthermore, it has been observed that there is a better coupling of N2fixation rates with BP rather than with PP in the eastern MS (Rahav et al., 2013b). This was also observed within the ML in this study. Our data showed that the hypothetical contribution of N2fixation rates to hprokN demand within the ML was low (6.4 ± 2.4%) and consistent with the low N2fixation rates observed in the MS (i.e Rahav et al., 2013a; Ibello et al., 2010; Ridame et al., 2011; Bonnet et al., 2011). This differs from other parts of the ocean primarily limited by N but not by P, such as the south eastern Pacific where N₂ fixation rates are high (Bonnet et al., 2017) and can represent up to 81 % of the hprokN demand (Van Wambeke et al., 2018).
- 940 The sum of LAP activity and N₂ fixation were not sufficient to meet hprokN demand (total contribution between 19 to 73% of HbactN demand). Finally, we examined the source of new DIN from dry atmospheric deposition. Atmospheric DIN fluxes from dry deposition presented a low variability along the transect (29 ± 7 µmol N m⁻² d⁻¹ at the short stations) and were among the lowest previously measured in the Mediterranean environment, ranging, from 38 to 240 µmol N m⁻² d⁻¹ (Desboeufs et al., in press). It has to be noted that the fluxes measured during the PEACETIME cruise are representative of the open sea atmosphere while published
- fluxes were measured at coastal sites where local/regional contamination contributes significantly to the flux (Desboeufs, in press). Atmospheric deposition also delivers organic matter (Djaoudi et al., 2017, Kanakidou et al., 2018), which is bioavailable for marine hprok
- 950 (Djaoudi et al., 2020). Dissolved organic nitrogen (DON) released from aerosols, not
 determined here, can be estimated from previous studies. <u>On average in the MS</u>, DON
 solubilized from aerosols <u>represents 32%</u>. <u>(range19 to 42%)</u> of the total dissolved N released
 from dry deposition (Desboeufs, in press), Considering this mean, DON released from dry
 deposition was estimated to range from 8 to 19 µmol N m⁻² d⁻¹ at the short duration stations.
- 955 The total dissolved N solubilized from dry deposition (inorganic measured +organic estimated) would thus represent 14 to 121% of the hprokN demand. Because of the low variability in DIN (and estimated DON) fluxes derived from dry deposition, the atmospheric contribution was mainly driven by biogeochemical conditions and not by the variability of atmospheric fluxes during the cruise (CV of Nprok Ndemand and phyto N demand at the
- 960 short stations were 45% and 89%, respectively, and that of DIN flux 25%). However, the calculated contribution can also be biased by the deposition velocity used to calculate DIN

Supprimé:

Supprimé: Considering LAP as the most relevant regeneration source of N, it is clear that Supprimé: even t Supprimé: cumulated, these fluxes Supprimé: contributed Supprimé: The last source of new N we examined was DIN released by Supprimé: Such Supprimé: such Supprimé: es

-	Supprimé: contributes
-{	Supprimé: in the MS
-	Supprimé: ,
М	Supprimé: with an average of 32%

solubilized from the dry deposition. Deposition velocity was set at 1 cm s⁻¹ for NO3 and 0.21 cm s⁻¹ for NH4. As NO3 was the dominant inorganic form released by dry deposition, it is clear that the choice of 1 cm s⁻¹ for NO3 influenced its contribution. This choice was conditioned by the predominance of NO3 in the large mode of Mediterranean aerosols such as dust or sea salt particles (e.g., Bardouki et al., 2003). However, the deposition velocity of NO3 between fine and large particles could range from 0.6 to 2 cm sec⁻¹ in the Mediterranean aerosols (e.g. Sandroni et al., 2007). Even considering the lower value of 0.6 cm sec⁻¹ from the literature, the contribution of DIN from atmospheric dry deposition to hprokN demand within the ML would still be significant (up to 72%).

985

980

4.2 Biogeochemical response after a wet <u>deposition</u> event – N and P budgets at FAST site

Rain events are more erratic than dry atmospheric deposition but represent on average much
higher new nutrient fluxes to the MS surface waters on an annual basis, e.g. 84% of annual
atmospheric DIN fluxes in Corsica Island (Desboeufs et al., 2018). <u>At the scale of the</u>
Mediterranean basin, the annual wet deposition of DIN was found to be 2-8 times higher than
DIN from dry deposition (Markaki et al., 2010). Wet deposition also contributes significantly
to DON atmospheric fluxes in the MS: For example at Frioul Island (Bay of Marseille, NW
995 MS), total (wet + dry) DON atmospheric fluxes ranged between 7 and 367 µmol DON m⁻²
day⁻¹ and represented 41 ± 14% of the total atmospheric nitrogen flux (Djaoudi et al., 2018). In the Eastern MS (Lampedusa Island) DON atmospheric fluxes ranged between 1.5 and 250
µmol DON m⁻² day⁻¹ contributing to 25% of the total atmospheric nitrogen flux, respectively (Galletti et al., 2020). In both studies, bulk atmospheric fluxes of DON were positively

1000 correlated with precipitation rates, indicating the preponderance of wet deposition over dry deposition.

At the FAST site, the maximum net variations of NO3 and DIP concentrations within the ML before/after the rainy period reached 1520-665 = +855 µmol N m⁻² for NO3 and 281-137 = +144 µmol P m⁻² for DIP (Table S2). In other terms, based on a mean MLD of 16 m, the net observed increases in the ML were + 9 nM DIP and + 54 nM NO3. These net variations observed in the ML are higher than the calculated variation in stocks deduced from the N and P concentrations of this rain event (0.07 nM DIP and 21 nM NO3 concentrations increase over the whole ML (Table 3). This is still true when including all P or N chemical forms
1010 (particulate and soluble inorganic + organic fractions). For example the P concentration in the

Supprimé: ec Supprimé: ec Supprimé: ec

Supprimé: On

Supprimé: As the rain event in the area would have increase by

Supprimé:

Supprimé: mixed layer, the net variations observed in the ML are thus higher than the calculated variation in stocks deduced from the N and P concentrations of this rain event ML would increase by ~0.68 nM. As described in the results section 3.4, the rains affecting the FAST site were spatially patchy over a large area (~40-50 km radius around the R/V).

- 1025 Thus, we consider that the biogeochemical impacts observed at FAST site were probably due to a suite of atmospheric events rather than <u>only</u> the single event <u>observed</u> on board. It is <u>also</u> possible that meso- and sub-mesoscale dynamics encountered at FAST site (Figs 5 and 12 in Guieu et al., 2020) <u>may have affected</u> such cumulative impact.
- Interestingly, a delay of about 19 h was observed in the maximum net accumulation within 1030 the ML between DIP (FAST+1.05) and NO3 (FAST+0.24). The DIN/DIP ratio in the rain (1438) was much higher than the Redfield ratio. As the biological turnover of DIP in the MS is rapid (from min<u>utes</u> to few h<u>ours</u>, Talarmin et al., 2015), new DIP from rain might have behaved differently than DIN. Two different mechanisms can explain this delay: (i) processes linked to bypasses and luxury DIP uptake (storage of surplus P in hprok before a rapid
- 1035 development of grazers (Flaten et al, 2005; Herut et al 2005, Thingstad et al., 2005) that are later responsible for DIP regeneration) so that DIP net accumulation is delayed and/or (ii) abiotic processes such as rapid desorption from large sinking particles followed by adsorption of DIP onto submicronic iron oxides still in suspension as observed experimentally in Louis et al. (2015).
- 1040 The first proposed mechanism may be supported by the observed increase of BP, along with a stable PP which suggests an immediate benefit of the new nutrients from rain by hprok rather than phytoplankton. The so-called luxury DIP uptake by the competing organisms like hprok is efficient (small cells with high surface/volume ratio and DIP kinetic uptake adapted to low concentrations). It is of course difficult to quantify such *in situ* variations in comparison to
- 1045 mesocoms/minicosms dust addition experiments, in which clearly heterotrophy is favoured first (Marañón et al., 2010; Guieu et al., 2014b; Gazeau et al., 2021). Few attempts in the field have confirmed these trends (Herut et al., 2005, Pulido-Villena et al., 2008) but, as stated in the introduction, these studies lacked high frequency sampling.
- The second proposed mechanism, the abiotic desorption/adsorption, is compatible with the 1050 observed 19 h delay (Louis et al., 2015). Note that most of the estimates of such abiotic processes are from dust addition experiments with contrasting results, some showing this abiotic process of absorption/desorption while the particles are sinking (Louis et al., 2015), and other not (Carbo et al., 2005) or showing it as negligible in batch experiments (Ridame et al., 2003). It is possible that DIP adsorbed onto large particles rapidly sinks out of the ML,

Supprimé: could
Supprimé: due to
Supprimé: collected
Supprimé: can
Supprimé: explain

1060	and desorbs partly during its transit in the PDLb, where it could stay longer thanks to the	
	pycnoclines barriers.	
	We made a tentative P budget between FAST+1.05 and FAST+2.11 where a net decrease of	 Supprimé: tentatively
	DIP (-87 μ mol P m ⁻²) was observed in the ML. During this time, advective flux of DIP toward	
	the PDLb was not detectable as DIP concentrations within the ML were always lower than	
1065	within the PDLb (Pulido-Villena et al., 2021.). This indicated that the DIP was assimilated	
	and/or transformed to DOP via biological processes, and/or adsorbed onto particles and then	
	exported to PDLb by sedimentation. By integration of PP and BP over this period (34.5 and	
	19.7 mg C m ⁻² , respectively) and, by assuming that all the disappearing 87 μmol DIP m ⁻²	
	would be consumed by hprok and phytoplankton, a C/P ratio reached in their biomass would	 Supprimé: we could estimate
1070	be 52. Such C/P suggests that DIP was not limiting these organisms anymore. Indeed a	Supprimé: of
	decrease of C/P quotas may highlight a switch from P to C limitation for heterotrophic	Supprimé: ((34.5+19.7)/12x1000)/87=
	bacteria (Godwin and Cotner, 2015) and from P to N limitation or increased growth rates for	
	phytoplankton (Moreno and Martiny, 2018). Furthermore, as DIP is also recycled via alkaline	
	phosphatase within the ML, we also consider another source of DIP via alkaline phosphatase	
1075	activity, from which in situ activity (see Van Wambeke et al., 2021 for in situ estimates)	
	could release 139 μ mol DIP m ⁻² during this period. Assuming also that DIP resulting from AP	 Supprimé: of
	hydrolysis was fully assimilated for P biological needs, then C/P ratio would be 19. This low	 Supprimé: (((34.5+19.7)/12x1000))/(87+ 139) =
I	ratio seems unrealistic for phytoplankton (Moreno and Martigny, 2018) as well as hprok, even	157)-
	growing in surplus C conditions (Makino et al., 2003; Lovdal et al., 2008; Godwin and	
1080	Cotner, 2015).	
	Some of the P recycled or brought into the ML from atmospheric deposition has consequently	
	been exported below the ML. DIP is abiotically adsorbed on mineral dust particles (Louis et	
	al., 2015), and constitute a source of export out of the ML while the particle sink. It is also	 Supprimé: most of them sinking,
I	possible that such sorbing process on dust particles enables the export of other P-containing	Supprimé: thus
1085	organic molecules, for instance DOP or viruses produced following luxury DIP assimilation.	
	Free viruses, richer in P than N relative to Hprok, could adsorb, like DOM, onto dust particles	
	and constitute a P export source. Indeed, free viruses adsorb onto black carbon particles,	
I	possibly reducing viral infection (Mari et al., 2019; Malits et al., 2015). However, particle	
	quality is a determining factor for DOM or microbial attachment, and what has been shown	
1090	for black carbon particles is not necessarily true for dust particles. For instance the addition of	
	Saharan dust to marine coastal waters led to a negligible sorption of viruses to particles and	
	increased abundance of free viruses (Pulido-Villena et al., 2014), possibly linked to an	

enhancement of lytic cycles in the ML after relieving limitation (Pradeep Ram and Sime-Ngando, 2010).

We are aware of all the assumptions made here, including (i) conversion factors, (ii) in situ
estimates of alkaline phosphatase, (iii) some missing DIP sources in the budget, such as the excretion of zooplankton estimated to amount to 22-37% of the phytoP demand at FAST site (Feliú et al., 2020), iv) lack of knowledge on the different mechanisms linking P to dust particles, and (iv) considering the station as a 1D system. Nevertheless, all these results together suggest that both luxury consumption by Hprok and export via scavenging on
mineral particles probably occurred simultaneously and could explain the observed variations of DIP in the ML.

For NO3, and in contrast to the observations for DIP, we observed physical exchanges by advection between the ML and NDLb. A N budget within the ML during the period of net
NO3 decrease (between FAST+0.24, and FAST+2.11, Table S2), indicates a net loss of 1343 µmol N m⁻². For this period lasting 1.8 days, the time-integrated phytoN and hprokN demands were 682 µmol N m⁻² and 378 µmol N m⁻², respectively, so that total biological demand in the ML was 1060 µmol N m⁻². During this period, the possible N sources used were net NO3 decrease assumed to be consumption = 1343 µmol N m⁻² as well as N₂ fixation = 13 µmol N m⁻² and *in situ* aminopeptidase activity = 87 µmol N m⁻². In total, the possible source of N amounted to 1443 µmol N m⁻². Keeping in mind that the same potential caveats pointed to DIP (see above) also apply for the calculation of N budget, the biological N demand appeared lower than the sources (difference ~380 µmol N m⁻²). On the other hand, at FAST site, vertical advective fluxes of NO3 from ML to NDLb were up to 337 µmol N m⁻² d⁻¹ (Fig. 4),

- i.e ~600 µmol N m⁻² was lost from the ML over 1.8 days. From these two different approaches, exported NO3 should range between 380 and 600 µmol N m⁻² over this period. Thus, about 40% of the NO3 accumulated in the ML after the rain was likely exported by vertical advection to the NDLb. Organisms present in the DCM could benefit of this input of new nutrients. Indeed, PP and abundances of all 4 phytoplankton groups (*Synechococcus*,
- 1130 *Prochlorococcus*, nano and picoeukaryotes) increased at the DCM after 24h and remained high for 2 days after the rain event (Fig. S3). The increase in abundances were higher for prokaryotic phytoplankton abundances, as such organisms would likely benefit from their small size and their ability to use DON/DOP organic molecules (Yelton et al., 2016).

Supprimé: (

Supprimé: the hypothesis which Supprimé: s

Supprimé: within the ML

Supprimé: were Supprimé: disappearing stocks of Supprimé: (net diminution Supprimé:), Supprimé: where fluxes integrated over this time period were 13 and Supprimé: , respectively

5. Conclusions

	This study reports for the first time, in the context of an oceanographic cruise, simultaneous							
1150	sampling of atmospheric and ocean biogeochemical parameters to characterize the in situ							
	biogeochemical responses to atmospheric deposition within the ML. High-frequency	Supprimé: the						
	sampling, in particular at the FAST site, confirmed the transitory state of exchanges between							
	the ML and the NDLb. Even if dry deposition measured along the transect was homogeneous							
	and amongst the lowest observed in the MS, that input could represent up to 121% of the	Supprimé: in						
I	hprokN demand. Furthermore, the signature of the dust wet deposition event on DIP and DIN							
	concentrations was clearly detected, considering both the local rain fluxes and the horizontal	Supprimé: emphasized						
1155	oceanic mixing of water masses affected by the rain front,	Supprimé: Finally, a comparison with						
	Our results have shown the important role played by the ML in the biogeochemical and	the mesocosms results (where the fertilization is more important due to high dust concentrations) is hard to extrapolate						
		with the data presented here.						
	physical processes responsible for transfers of nutrients between the atmosphere and the	Supprimé: matter and						
	nutrient depleted layer below. Thanks to the use of the LWCC technique and access to							
	nanomolar variations of NO3 and DIP in repeated CTD casts, it was possible to demonstrate							
1160	the role of the ML and exchanges of NO3 from the ML to the NDLb by vertical advection							
	when variations of MLD occurred simultaneously to transitory accumulation of NO3 after a							
	deposition event. The time sequence occurring after a wet dust deposition event was							
	summarized as follows (Fig. 6): accumulation of NO3 in the ML, advection to NDLb, luxury							
	consumption of DIP by hprok and delayed peaks of DIP, decrease of primary production and							
1165	subsequent recovery after 2 days, mainly visible in the nutrient depleted layer. Dust	Supprimé: its						
	deposition triggers a complex and time-controlled trophic cascade within the microbial food	Supprimé: The effect of d						
	web. Our study shows the important role of intermittent, but strong abiotic effects such as	Supprimé: is						
	downwelling advective fluxes from the ML to the nutrient depleted layers. It will be							
	important to consider these aspects in <u>biogeochemical</u> budgets and models, especially when	Supprimé: o						
1170	climate and anthropogenic changes are predicted to increase aerosol deposition in the	Supprimé: non-stoichiometric						
11,5	Mediterranean Sea.							
	Data availability							

Data availability

Guieu et al., Biogeochemical dataset collected during the PEACETIME cruise. SEANOE. https://doi.org/10.17882/75747 (2020).

1175

Author contribution

CG and KD designed the study. FVW measured ectoenzymatic activity and BP, AE managed the TAA analysis and treatments, EP measured DIP with the LWCC technique, CR measured nitrogen fixation, VT assisted in CTD operations and analyzed water masses, JD sampled for DOC and flow cytometry, <u>EM analyzed the primary production</u> <u>data</u>, FVW prepared the ms with contribution from all co-authors.

1195

1210

Competing interests

The authors declare that they have no conflict of interest.

1200 Special issue statement

This article is part of the special issue 'Atmospheric deposition in the low-nutrient-lowchlorophyll (LNLC) ocean: effects on marine life today and in the future (ACP/BG interjournal SI)'. It is not associated with a conference.

1205 Financial support

The project leading to this publication received funding from CNRS-INSU, IFREMER, CEA, and Météo-France as part of the program MISTRALS coordinated by INSU (doi: 10.17600/17000300) and from the European FEDER fund under project no 1166-39417. The research of EM was funded by the Spanish Ministry of Science, Innovation and Universities through grant PGC2018-094553B-I00 (POLARIS).

	Acknowledgements. This study is a contribution of the PEACETIME project
	(http://peacetime-project.org, last access 13/07/2021), a joint initiative of the MERMEX
I	and ChArMEx components. PEACETIME was endorsed as a process study by
1215	GEOTRACES and is also a contribution to IMBER and SOLAS international programs.
	The authors thank also many scientists & engineers for their assistance with
	sampling/analyses: Samuel Albani for NO3 nanomolar sampling and Maryline Montanes for
	NO3 with LWCC technique, Marc Garel, Sophie Guasco and Christian Tamburini for
	ectoenzymatic activity, Ruth Flerus and Birthe Zancker for TAA, Joris Guittoneau and Sandra
1220	Nunige for nutrients, Thierry Blasco for POC, Julia Uitz and Céline Dimier for TChl a
	(analysed at the SAPIG HPLC analytical service at the IMEV, Villefranche), María Pérez
	Lorenzo for primary production measurements, Philippe Catala for flow cytometry analyses,
I	Barbara Marie and Ingrid Obernosterer for DOC analyses and treatments. Sylvain Triquet and

Supprimé: 07 Supprimé: 04 Franck Fu for atmospheric particulate nitrogen and phosphorus<u>and PEGASUS team for</u> <u>atmospheric sampling</u>. Maurizio Ribera d'Alcala and a second anonymous reviewer helped much to improve this ms.

1230 References

1235

1240

1250

- Aminot, A., and Kérouel, R. : Dosage automatique des nutriments dans les eaux marines, in: Méthodes d'analyses en milieu marin, edited by: IFREMER, Plouzané, 188 pp, IBSN no 978-2-7592-0023-8, 2007.
- Bardouki, H., Liakakou, H., Economou, C., Sciare, J., Smolik, J., Zdimal, V., Eleftheriadis,K., Lazaridis, M., Dye, C., and Mihalopoulos, N.: Chemical composition of size
- resolved atmospheric aerosols in the eastern Mediterranean during summer and winter, Atmos. Environ., 37, 195–208, 2003.
- Bonnet, S., Grosso, O., and Moutin, T.: Planktonic dinitrogen fixation along a longitudinal gradient across the Mediterranean Sea during the stratified period (BOUM cruise),
 Biogeosciences, 8, 2257–2267, 2011.
- Bonnet, S., Caffin, M., Berthelot, H., and Moutin, T.: Hot spot of N₂ fixation in the western tropical South Pacific pleads for a spatial decoupling between N2 fixation and denitrification, PNAS letter, doi: 10.1073/pnas.1619514114, 2017.
- Caffin, M., Berthelot, H., Cornet-Barthaux, V., Barani, A., and Bonnet, S.: Transfer of
 diazotroph-derived nitrogen to the planktonic food web across gradients of N₂ fixation activity and diversity in the western tropical South Pacific Ocean, Biogeosciences, 15, 3795–3810, doi: 10.5194/bg-15-3795-2018, 2018.
 - Carbo, P., Krom, M. D., Homoky, W. B., Benning, L. G., and Herut, B.: Impact of atmospheric deposition on N and P geochemistry in the southeastern Levantine basin, Deep Sea Res. II, 52, 3041–3053. doi: 10.1016/j.dsr2.2005.08.014, 2005.
 - Céa, B., Lefèvre, D., Chirurgien, L., Raimbault, P., Garcia, N., Charrière, B., Grégori, G.,Ghiglione, J.-F., Barani, A., Lafont, M., and Van Wambeke, F.: An annual survey ofbacterial production, respiration and ectoenzyme activity in coastal NW Mediterranean

Supprimé: Brainerd, K. E., and Gregg, M. C.: Surface mixed and mixing layer depths, Deep-Sea Research Part I, 42(9), 1521–1543. doi: 10.1016/0967-0637(95)00068-H, 1995.¶ waters: temperature and resource controls, Environ. Sci. Pollut. Res., doi: 10.1007/s11356-014-3500-9, 2014.

1260

- Christaki, U., Courties, C., Massana, R., Catala, P., Lebaron, P., Gasol, J. M., and Zubkov,M.: Optimized routine flow cytometric enumeration of heterotrophic flagellates usingSYBR Green I, Limnol. Oceanogr. Methods, 9, doi: 10.4319/lom.2011.9.329, 2011.
- Cullen, J. J., Franks, P. J., Karl, D. M., and Longhurst, A. L. A. N.: Physical influences onmarine ecosystem dynamics. The sea, 12, 297-336, 2002.
 - de Boyer Montegut, C., Madec, G., Fisher, A. S., Lazar, A., and Iudicone, D.: Mixed layer depth over the global ocean: An examination of profile data and a profile-based climatology, Journal of Geophysical Research. Oceans, 109, C12003, doi: 10.1029/2004JC002378, 2004.
- 1270 Delmont, T. O., Quince, C., Shaiber, A., Esen, Ö. C., Lee, S. T. M., Rappé, M. R., McLellan, S. L, Lücker, S. and Murat Eren, A.: Nitrogen-fixing populations of Planctomycetes and Proteobacteria are abundant in surface ocean metagenomes, Nature Microbiology, doi: 10.1038/s41564-018-0176-9, 2018.
 - Desboeufs, K.: Nutrients atmospheric deposition and variability, in: Atmospheric Chemistry and its Impacts in the Mediterranean Region (ChArMex book), Springer, in press.
 - Desboeufs, K., Bon Nguyen, E., Chevaillier, S., Triquet, S., and Dulac, F.: Fluxes and sources of nutrient and trace metal atmospheric deposition in the northwestern Mediterranean, Atmospheric Chemistry and Physics, 18, 14477–14492, doi: 10.5194/acp-18-14477-2018, 2018.
- Desboeufs, K., Fu, F., Bressac, M., Tovar-Sánchez, A., Triquet, S., Doussin, J-F., Giorio, C.,
 <u>Chazette, P., Disnaquet, J., Feron, A., Formenti, P., Maisonneuve, P.,</u> Rodriguez-Roméro, A., Wagener, T., Dulac, F., and Guieu, C.: Wet deposition in the remote
 <u>western</u> and central Mediterranean Sea: A source <u>of trace metals to surface seawater</u>?,
 Atmos. Phys. Chem., this special issue, in preparation.
- 1285 Dittmar, T.H., Cherrier, J., and Ludwichowski, K.-U: The analysis of amino acids in seawater. In: Practical Guidelines for the Analysis of Seawater, edited by: Wurl, O., Boca Raton, FL: CRC-Press, 67–78, 2009.

Supprimé: a
Supprimé: Siour, G.,
Supprimé: of nutrients and trace metals
Supprimé: Western
Supprimé: for marine biosphere

- D'Ortenzio, F., Iudicone, D., de Boyer Montegut, C., Testor, P., Antoine, D., Marullo, S.,
 Santoleri, R., and Madec, G.: Seasonal variability of the mixed layer depth in the
 Mediterranean Sea as derived from in situ profiles., Geophysical Research Letters, 32,
 L12605, doi:10.1029/2005GL022463, 2005.
 - Djaoudi, K., Van Wambeke, F., Barani, A., Hélias-Nunige, S., Sempéré, R., and Pulido-Villena, E.: Atmospheric fluxes of soluble organic C, N, and P to the Mediterranean Sea: potential biogeochemical implications in the surface layer, Progress in Oceanography, 163: 59-69, MERMEX special issue, doi: 10.1016/j.pocean.2017.07.008, 2017.
 - Djaoudi, K., Van Wambeke, F., Coppola, L., D'ortenzio, F., Helias-Nunige, S., Raimbault, P., Taillandier, V., Testor, P., Wagener, T., and Pulido-Villena, E.: Sensitive determination of the dissolved phosphate pool for an improved resolution of its vertical variability in the surface layer: New views in the P-depleted Mediterranean Sea, Frontiers in Marine Science, vol 5, article 234, doi: 10.3389/fmars.2018.00234, 2018.
 - Djaoudi, K., Van Wambeke, F., Barani, A., Bhairy, N., Chevaillier, S., Desboeufs, K., Nunige, S., Labiadh, M., Henry des Tureaux, T., Lefèvre, D., Nouara, A.,
 Panagiotopoulos, C., Tedetti, M., and Pulido-Villena E.: Potential bioavailability of organic matter from atmospheric particles to marine heterotrophic bacteria, Biogeosciences, 17, 6271–6285, https://doi.org/10.5194/bg-17-6271-2020, 2020
 - Du, C., Liu, Z., Kao, S.-J., and Dai, M.: Diapycnal fluxes of nutrients in an oligotrophic oceanic regime: The South China Sea, Geophysical Research Letters, 44, 11, 510–11, 518, doi: 10.1002/2017GL074921, 2017.
- Feliú, G., Pagano, M., Hidalgo, P., and Carlotti, F.: Structure and function of epipelagic mesozooplankton and their response to dust deposition events during the spring PEACETIME cruise in the Mediterranean Sea, Biogeosciences, 17, 5417–5441, https://doi.org/10.5194/bg-17-5417-2020,2020.

Flaten, G. A., Skjoldal, E. F., Krom, M. D., Law, C. S., Mantoura, F. C., Pitta, P., Psarra, S.,
Tanaka, T., Tselepides, A., Woodward, E. M., Zohary, T., and Thingstad, T. F.: Studies of the microbial P-cycle during a Lagrangian phosphate-addition experiment in the Eastern Mediterranean, Deep-Sea Res II, 52, 2928–2943, 2005.

Supprimé:

1305

1310

Fu, F., Desboeufs, K., Triquet, S., Doussin, J-F., Giorio, C., and Guieu, C.: Solubility and sources of trace metals associated with aerosols collected during cruise PEACETIME in the Mediterranean Sea, Atmos. Phys. Chem., this special issue, in preparation.

1325

1330

1345

- Galletti, Y., Becagli, S., di Sarra, A., Gonnelli, M., Pulido-Villena, E., Sferlazzo, D. M., Traversi, R., Vestri, S., and Santinelli, C.: Atmospheric deposition of organic matter at a remote site in the Central Mediterranean Sea: implications for marine ecosystem, Biogeosciences, 17, 3669–3684, https://doi.org/10.5194/bg-17-3669-2020, 2020.
- Gasol, J. M., and del Giorgio, P. A.: Using flow cytometry for counting natural planktonic bacteria and understanding the structure of planktonic bacterial communities, Scientia Marina, 64, 197–224, 2000.
- Gazeau, F., Van Wambeke, F., Marañon, E., Pérez-Lorenzo, M., Alliouane, S., Stolpe, C.,
 Blasco, T., Leblond, N., Zäncker B., Engel A., Marie, B., Dinasquet, J., and Guieu C.: Impact of dust addition on the metabolism of Mediterranean plankton communities and carbon export under present and future conditions of pH and temperature,
 Biogeosciences Discuss. [preprint], https://doi.org/10.5194/bg-2021-20, in review, 2021.
- 1340 Godwin, C. M., and Cotner, J. B.: Aquatic heterotrophic bacteria have highly flexible phosphorus content and biomass stoichiometry, the ISME Journal, 9, 2324–2327, doi:10.1038/ismej.2015.34, 2015.
 - Guieu, C., and Ridame, C.: Impact of atmospheric deposition on marine chemistry and biogeochemistry, in: Atmospheric Chemistry and its Impacts in the Mediterranean Region (ChArMex book), Springer, in press.
- Guieu, C., Dulac, F., Desboeufs, K., Wagener, T., Pulido-Villena, E., Grisoni, J.-M., Louis, J., Ridame, C., Blain, S., Brunet, C., Bon Nguyen, E., Tran, S., Labiadh, M., and Dominici, J.-M.: Large clean mesocosms and simulated dust deposition: a new methodology to investigate responses of marine oligotrophic ecosystems to atmospheric inputs,
 Biogeosciences, 7, 2765–2784, doi: 10.5194/BG-7-2765-2010, 2010.
 - Guieu, C., Aumont, O., Paytan, A., Bopp, L., Law, C. S., Mahowald, N., Achterberg, E. P.,Marañón, E., Salihoglu, B., Crise, A., Wagener, T., Herut, B., Desboeufs, K.,Kanakidou, M., Olgun, N., Peters, F., Pulido-Villena, E., Tovar-Sanchez, A., and

Supprimé: Dulac, F.,

Supprimé: and nutrients

Supprimé: Gardner, W. D., Chung, S. P., Richardson, M. J., and Walsh, I. D.: The oceanic mixed-layer pump, Deep-Sea Research II 42, 757-775, 1995.¶

Supprimé:

Völker, C.: The significance of episodicity in atmospheric deposition to Low Nutrient Low Chlorophyll regions, Global Biogeochem. Cycles, 28, 1179–1198, doi:10.1002/2014GB004852, 2014a.

- Guieu, C., Ridame, C., Pulido-Villena, E., Bressac, M., Desboeufs, K., and Dulac, F.: Impact
 of dust deposition on carbon budget: a tentative assessment from a mesocosm approach, Biogeosciences, 11, 5621–5635, doi: 10.5194/bg-11-5621-2014, 2014b.
 - Guieu, C., D'Ortenzio, F., Dulac, F., Taillandier, V., Doglioli, A., Petrenko, A., Barrillon, S.,Mallet, M., Nabat, P., and Desboeufs, K.: Process studies at the air-sea interface after atmospheric deposition in the Mediterranean Sea: objectives and strategy of the
- 1370PEACETIME oceanographic campaign (May–June 2017), Biogeosciences, 17, 1–23,
2020, doi: 10.5194/bg-17-1-2020.
 - Heimburger, A., Losno, R., Triquet, S., Dulac F., and Mahowald, N. M.: Direct measurements of atmospheric iron, cobalt and aluminium-derived dust deposition at Kerguelen Islands, Global Biogeochem. Cy., 26, GB4016, doi:10.1029/2012GB004301, 2012.
- Hersbach, H., Bell, B., Berrisford, P., Biavati, G., Horányi, A., Muñoz Sabater, J., Nicolas, J.,
 Peubey, C., Radu, R., Rozum, I., Schepers, D., Simmons, A., Soci, C., Dee, D.,
 Thépaut, J-N.: ERA5 hourly data on single levels from 1979 to present. Copernicus
 Climate Change Service (C3S) Climate Data Store (CDS). doi: 10.24381/cds.adbb2d47, 2018.
- Herut, B., Zohary, T., Krom, M. D., Mantoura, R. F. C., Pitta, P., Psarra, S., Rassoulzadegan,
 F., Tanaka, T. and Thingstad, T. F.: Response of East Mediterranean surface water to
 Saharan dust: On-board microcosm experiment and field observations, Deep-Sea
 Research II 52 (2005) 3024–3040, 2005.
- Herut, B., Rahav, E., Tsagaraki, T. M., Giannakourou, A., Tsiola, A., Psarra, S., Lagaria, A.,
 Papageorgiou, N., Mihalopoulos, N., Theodosi, C. N., Violaki, K., Stathopoulou, E.,
 Scoullos, M., Krom, M. D., Stockdale, A., Shi, Z., Berman-Frank, I., Meador, T. B.,
 Tanaka, T., and Paraskevi, P.: The potential impact of Saharan dust and polluted
 aerosols on microbial populations in the East Mediterranean Sea, an overview of a
 mesocosm experimental approach, Front. Mar. Sci, 3, 226, doi:
- 1390 10.3389/fmars.2016.00226, 2016.

- Hoppe, H.-G., Ducklow, H., and Karrasch, B.: Evidence for dependency of bacterial growth on enzymatic hydrolysis of particulate organic matter in the mesopelagic ocean, Mar. Ecol. Prog. Ser., 93, 277–283, 1993.
- Ibello, V., Cantoni, C., Cozzi, S., and Civitarese, G.: First basin-wide experimental results on N2 fixation in the open Mediterranean Sea, Geophys. Res. Lett., 37, L03608, doi:10.1029/2009GL041635, 2010.

- Izquierdo, R., Benítez-Nelson, C. R., Masqué, P., Castillo, S., Alastuey, A., and Àvila, A.: Atmospheric phosphorus deposition in a near-coastal rural site in the NE Iberian Peninsula and its role in marine productivity, Atmos. Environ., 49, 361–370,doi: 10.1016/j.atmosenv.2011.11.007, 2012.
- Jumars, P. A., Penry, D. L., Baross, J. A., Perry, M. A., and Frost, B. W.: Closing the microbial loop : dissolved carbon pathway to heterotrophic bacteria from incomplete ingestion, digestion and absorption in animals, Deep-Sea Research, 483–495, 1989.
- Kamykowski, D., and Zentara, S. J.: Nitrate and silicic acid in the world ocean: Patterns and processes, Mar. Ecol. Prog. Ser., 26, 47–59, 1985.
 - Kanakidou, M., Myriokefalitakis, S., and Tsigaridis, K.: Aerosols in atmospheric chemistry and biogeochemical cycles of nutrients, Environ. Res. Lett., 13, 063004, doi: 10.1088/1748-9326/aabcdb, 2018.
- Kanakidou, M., Myriokefalitakis, S., and Tsagkaraki, M.: Atmospheric inputs of nutrients to
 the Mediterranean Sea, Deep Sea Research Part II: Topical Studies in Oceanography,
 171, 104606, doi: 10.1016/j.dsr2.2019.06.014, 2020.
 - Kirchman, D. L.: Leucine incorporation as a measure of biomass production by heterotrophic bacteria, in: Handbook of methods in aquatic microbial ecology, edited by : Kemp, P.F., Sherr, B.F., Sherr, E.B., and Cole, J.J., Lewis, Boca Raton, 509-512, 1993.
- Kouvarakis, G., Mihalopoulos, N., Tselepides, T., and Stavrakakis, S.: On the importance of atmospheric nitrogen inputs on the productivity of eastern Mediterranean, Global Biogeochemical Cycles, 15, 805–818, doi:10.1029/2001GB001399, 2001.

Krom, M. D., Herut, B., and Mantoura, R. F. C.: Nutrient budget for the eastern Mediterranean: Implication for phosphorus limitation, Limnol. Oceanogr, 49, 1582– 1592, doi: 10.4319/lo.2004.49.5.1582, 2004.

1420

1430

- Louis, J., Bressac, M., Pedrotti, M.-L., and Guieu, C.: Dissolved inorganic nitrogen and phosphorus dynamics in sea water following an artificial Saharan dust deposition event, Frontiers Marine Sci., 2, article 27, doi: 10.3389/fmars.2015.00027, 2015.
- Løvdal, T., Skjoldal, E. F., Heldal, M., Norland, S., and Thingstad, T. F.: Changes in
 Morphology and Elemental Composition of Vibrio splendidus Along a Gradient from Carbon-limited to Phosphate-limited Growth, Microb. Ecol., 55, 152–161, doi: 10.1007/s00248-007-9262-x, 2008.
 - Makino, W., Cotner, J. B., Sterner, R. W., and Elser, J. J.: Are bacteria more like plants or animals? Growth rate and resource dependence of bacterial C : N : P stoichiometry, Functional Ecology, 17, 121–130, 2003.
 - Malits, A., Cattaneo, R., Sintes, E., Gasol, J. M., Herndl, G. J., and Weinbauer, M.: Potential impacts of black carbon on the marine microbial community, Aquat Microb Ecol., 75, 27–42, doi: 10.3354/ame01742, 2015.
 - Marañón, E., Fernández, A., Mouriño-Carballido, B., Martínez-García, S., Teira, E.,
- 1435 Cermeño, P., Chouciño, P., Huete-Ortega, M., Fernández, E., Calvo-Díaz, A., Morán,
 X. A. G., Bode, A., Moreno-Ostos, E., Varela, M. M., Patey, M. D., and Achterberg, E.
 P.: Degree of oligotrophy controls the response of microbial plankton to Saharan dust,
 Limnology and Oceanography, 55, 2339–2352, 2010.
- Marañón, E., Van Wambeke, F., Uitz, J., Boss, E. S., Dimier, C., Dinasquet, J., Angel, A.,
 Haëntjens, N., Pérez-Lorenzo, M., Taillandier, V., and Zäncker, B.: Deep maxima of phytoplankton biomass, primary production and bacterial production in the Mediterranean Sea, Biogeosciences, 18, 1749-1767, doi:10.5194/bg-18-1749-2021, 2021.
- Mari, X., Guinot, B., Chu, V. T., Brune, J., Lefebvre, J.-P., Pradeep Ram, A. S., Raimbault,
 P., Dittmar, T., and Niggemann, J.: Biogeochemical Impacts of a Black Carbon Wet
 Deposition Event in Halong Bay, Vietnam, Front. Mar. Sci, 6, article 185, doi:
 10.3389/fmars.2019.00185, 2019.

- Marie, D., Simon, N., Guillou, L., Partensky, F., and Vaulot, D.: Flow Cytometry Analysis of Marine Picoplankton, in: In Living Color: Protocols in Flow Cytometry and Cell
 Sorting, edited by: Diamond, R. A., and Demaggio, S., Springer, Berlin, Heidelberg, 421–454, 2000.
 - Markaki, Z., Loye-Pilot, M. D., Violaki, K., Benyahya, L., and Mihalopoulos, N.: Variability of atmospheric deposition of dissolved nitrogen and phosphorus in the Mediterranean and possible link to the anomalous seawater N/P ratio, Marine Chemistry, 120, 187– 194, doi: 10.1016/j.marchem.2008.10.005, 2010.

1465

- Martiny, A. C., Pham, C. T. A., Primeau, F. W., Vrugt, J. A., Moore, J. K., Levin, S. A., and Lomas, M. W.: Strong latitudinal patterns in the elemental ratios of marine plankton and organic matter, Nature geosciences, 6, 279–283, doi: 10.1038/ngeo1757, 2013.
- Mermex Group.: Marine ecosystems' responses to climatic and anthropogenic forcings in the Mediterranean, Progress in Oceanography, 91, 97–166, doi: 10.1016/j.pocean.2011.02.003, 2011.
 - Mescioglu E., Rahav E., Frada M.J., Rosenfeld S., Raveh O., Galletti Y., Santinelli C., Herut B., Paytan A.: Dust-associated airborne microbes affect primary and bacterial production rates, and eukaryote diversity, in the Northern Red Sea: A mesocosm approach. Atmosphere, 10, article 358, doi: 10.3390/atmos10070358, 2019.
 - Moreno, A. R., and Martiny, A. C.: Ecological stoichiometry of ocean plankton, Ann. Rev. Mar. Sci., 10, 43–69, 2018.
 - Nagata, T.: Carbon and Nitrogen content of natural planktonic bacteria, Appl., Environ. Microbiol., 52, 28–32, 1986.
- 1470 Orsini, D., Ma, Y., Sullivan, A., Sierau, B., Baumann, K., and Weber, R.: Refinements to the Particle-Into-Liquid Sampler (PILS) for Ground and Airborne Measurements of Water Soluble Aerosol Composition, Atmospheric Environment, 37, 1243–1259, 2003.
 - Omand, M. M. and Mahadevan, A.: The shape of the oceanic nitracline, Biogeosciences, 12, 3273–3287, doi: 10.5194/bg-12-3273-2015, 2015.

Supprimé: Moutin, T., and Prieur, L.: Influence of anticyclonic eddies on the Biogeochemistry from the Oligotrophic to the Ultraoligotrophic Mediterranean (BOUM cruise), Biogeosciences, 9 (10), 3827 – 3855, doi: 10.5194/bg-9-3827-2012, 2012.¶

- Pradeep Ram, A. S., and Sime-Ngando, T.: Resources drive trade-off between viral lifestyles in the plankton: evidence from freshwater microbial microcosms, Environ Microbiol, 12, 467–479, doi: 10.1111/j.1462-2920.2009.02088.x, 2010.
- Prieur, L., D'Ortenzio, F., Taillandier, V. and Testor, P.: Physical oceanography of the

 Ligurian sea. In: Migon C., Sciandra A. & Nival P. (eds.), the Mediterranean sea in the

 era of global change (volume 1), evidence from 30 years of multidisciplinary study of

 the Ligurian sea, ISTE Sci. Publ. LTD, 49–78. doi:10.1002/9781119706960.ch3,

 2020.
- Pujo-Pay, M., and Raimbault, P.: Improvements of the wet-oxidation procedure for simultaneous determination of particulate organic nitrogen and phosphorus collected on filters, Mar. Ecol. Prog. Ser., 105, 203–207, 1994,
 - Pulido-Villena, E., Wagener, T., and Guieu, C.: Bacterial response to dust pulses in the western Mediterranean: Implications for carbon cycling in the oligotrophic ocean, Global Biogeochem. Cycles, 22, GB1020, doi:10.1029/2007GB003091, 2008.
 - Pulido-Villena, E., Rérolle, V., and Guieu, C.: Transient fertilizing effect of dust in Pdeficient surface LNLC ocean. Geophysical Research Letters, 37, L01603, doi:10.1029/2009GL041415, 2010.

- Pulido-Villena, E., Baudoux, A.-C., Obernosterer, I., Landa, M., Caparros, J., Catala, P.,
 Georges, C., Harmand, J., and Guieu, C.: Microbial food web dynamics in response to a Saharan dust event: results from a mesocosm study in the oligotrophic Mediterranean Sea, Biogeosciences, 11, 337–371, 2014.
- Pulido-Villena, E., Desboeufs, K., Djaoudi, K., Van Wambeke, F., Barrillon, S., Doglioli, A., Petrenko, A., Taillandier, V., Fu, F., Gaillard, T., Guasco, S., Nunige, S., Triquet, S., and Guieu, C.: Phosphorus cycling in the upper waters of the Mediterranean Sea (Peacetime cruise): relative contribution of external and internal sources, Bigeosciences Discuss., [preprint], https://doi.org/10.5194/bg-2021-94, in review, 2021.
- Rahav, E. Herut, B., Levi, A., Mulholland, M. R., and Berman-Frank, I.: Springtime
 contribution of dinitrogen fixation to primary production across the Mediterranean
 Sea. Ocean Sci. 9, 489–498. doi: 10.5194/os-9-489-2013, 2013a

Supprimé: ¶

Rahav, E., Herut, B., Stambler, N., Bar-Zeev, E. Mulholland, M. R., and Berman-Frank, I.: Uncoupling between dinitrogen fixation and primary productivity in the eastern
Mediterranean Sea, J. Geophys. Res. Biogeosci., 118, 195–202, doi:10.1002/jgrg.20023, 2013b.

1515

1520

- Rahav, E., Paytan, A., Chien, C.-T., Ovadia, G., Katz, T., and Herut, B.: The Impact of Atmospheric Dry Deposition Associated Microbes on the Southeastern Mediterranean Sea Surface Water following an Intense Dust Storm, Front. Mar. Sci, 3, 127, doi: 10.3389/fmars.2016.00127, 2016.
- Richon, C., Dutay, J. C., Dulac, F., Wang, R., Balkanski, Y., Nabat, P., Aumont, O.,
 Desboeufs, K., Laurent, B., Guieu, C., Raimbault, P., and Beuvier, J.: Modeling the impacts of atmospheric deposition of nitrogen and desert dust-derived phosphorus on nutrients and biological budgets of the Mediterranean Sea, Prog. Oceanogr, 163, 21–39, doi: 10.1016/j.pocean.2017.04.009, 2018.
 - Ridame, C., Moutin, T., and C. Guieu.: Does phosphate adsorption onto Saharan dust explain the unusual N/P ratio in the Mediterranean Sea? Oceanologica Acta, 26, 629–634, doi: 10.1016/S0399-1784(03)00061-6, 2003.
- Ridame, C., Le Moal, M., Guieu, C. Ternon, E., Biegala, I., L'Helguen, S., and Pujo-Pay, M.: Nutrient
 control of N₂ fixation in the oligotrophic Mediterranean Sea and the impact of Saharan dust
 events, Biogeosciences, 8, 2773–2783, doi:10.5194/bg-8-2773-2011, 2011.
 - Sala, M. M., Peters, F., Gasol, J. M., Pedros-Alio, C., Marrasse, C., and Vaque, D.: Seasonal and spatial variations in the nutrient limitation of bacterioplankton growth in the northwestern Mediterranean, Aquat. Microb. Ecol., 27, 47–56, 2002.
- 1535 Sandroni, V., Raimbault, P., Migon, C., Garcia, N., and Gouze, E.: Dry atmospheric deposition and diazotrophy as sources of new nitrogen to northwestern Mediterranean oligotrophic surface waters, Deep-Sea Res. I, 54, 1859–1870, doi:10.1016/j.dsr.2007.08.004, 2007.
- Taillandier, V., Prieur, L., D'Ortenzio, F., Ribera d'Alcala, M., and Pulido-Villena, E.:
 Profiling float observation of thermohaline staircases in the western Mediterranean Sea and impact on nutrient fluxes, Biogeosciences, 17, 3343–3366, 2020.

- Talarmin A, Van Wambeke F., Lebaron P., and Moutin T.: Vertical partitioning of phosphate uptake among picoplankton groups in the low Pi Mediterranean Sea, Biogeosciences, 12: 1237–1247 doi:10.5194/bg-12-1237-2015, 2015.
- 1545 Tanaka, T., Thingstad, T. F., Christaki, U., Colombet, J., Cornet-Barthaux, V., Courties, C., Grattepanche, J.-D., Lagaria, A., Nedoma, J., Oriol, L., Psarra, S., Pujo-Pay, M., and Van Wambeke, F.: Lack of P-limitation of phytoplankton and heterotrophic prokaryotes in surface waters of three anticyclonic eddies in the stratified Mediterranean Sea, Biogeosciences, 8, 525–538, doi: 10.5194/bg-8-525-2011, 2011.
- 1550 Tovar-Sánchez, A., Rodríguez-Romero, A., Engel, A., Zäncker, B., Fu, F., Marañón, E., Pérez-Lorenzo, M., Bressac, M., Wagener, T., Triquet, S., Siour, G., Desboeufs, K., and Guieu, C.: Characterizing the surface microlayer in the Mediterranean Sea: trace metal concentrations and microbial plankton abundance, Biogeosciences, 17, 2349–2364, https://doi.org/10.5194/bg-17-2349-2020, 2020.
- Thingstad, T., Krom, M. D., Mantoura, F., Flaten, G., Groom, S., Herut, B., Kress, N., Law,
 C. S., Pasternak, A., Pitta, P., Psarra, S., Rassoulzadegan, F., Tanaka, T., Tselepides,
 A., Wassmann, P., Woodward, M., Riser, C., Zodiatis, G., and Zohary, T.: Nature of
 phosphorus limitation in the ultraoligotrophic eastern Mediterranean, Science, 309,
 1068–1071, doi: 10.1126/science.1112632, 2005.
- 1560 Van Wambeke, F., Christaki, U., Giannakourou, A., Moutin, T., and Souvemerzoglou, K.: Longitudinal and vertical trends of bacterial limitation by phosphorus and carbon in the Mediterranean Sea, Microb. Ecol., 43, 119–133, doi: 10.1007/s00248-001-0038-4, 2002.
- Van Wambeke, F., Gimenez, A., Duhamel, S., Dupouy, C., Lefevre, D., Pujo-Pay, M., and
 Moutin, T.: Dynamics and controls of heterotrophic prokaryotic production in the
 western tropical South Pacific Ocean: links with diazotrophic and photosynthetic
 activity, Biogeosciences, 15: 2669–2689, doi: 10.5194/bg-15-2669-2018, 2018.

Van Wambeke, F., Pulido-Villena, E., Catala, P., Dinasquet, J., Djaoudi, K., Engel, A., Garel,
 M., Guasco, S., Marie, B., Nunige, S., Taillandier, V., Zäncker, B., and Tamburini, C.:
 Spatial patterns of ectoenzymatic kinetics in relation to biogeochemical properties in

the Mediterranean Sea and the concentration of the fluorogenic substrate used, Biogeosciences, 18, 2301-2323, doi:10.5194/bg-18-2301-2021, 2021.

- Yelton, A. P., Acinas, S. G., Sunagawa, S., Bork, P., Pedros-Alio, C., Chisholm, S. W.: Global genetic capacity for mixotrophy in marine picocyanobacteria, ISME J 10:2946-2957, 2016.
- 1575
- Zhang, J.-Z., and Chi, J.: Automated analysis of nano-molar concentrations of phosphate in natural waters with liquid waveguide, Environ. Sci. Technol., 36, 1048–1053, doi : 10.1021/es011094v, 2002.

1580
 Table 1. Main biogeochemical features/trophic conditions during the PEACETIME cruise.
 For TYR, ION and FAST sites investigated over several days, means ± sd are indicated. ITChla: Integrated total chlorophyll a (Chla + dvChla). IPP: Integrated particulate primary production; IBP: integrated heterotrophic prokaryotic production. Integrations from surface to 200 m depth for all data expect IPP, integrated down to the depth of 1% Photosynthetically AR) level.

1585	Active Radiation	(PA)
------	------------------	------

		sampling date	Lat. °N	Long. °E	Temp. at 5 m °C	Bottom depth m	DCM depth m	ITChl a mg chla m ⁻²	IPP mg C m ⁻² d ⁻¹	IBP mg C m ⁻² d ⁻¹	
	ST1	May 12	41°53.5	6°20	15.7	1580	49	35 <u>.</u> 0	284	51	Supprimé: ,
	ST2	May 13	40°30.36	6°43.78	17.0	2830	65	32.7	148	55	 Supprimé: ,
	ST3	May 14	39°0.8.0	7°41.0	14.3	1404	83	23.2	140	77	 Supprimé: ,
	ST4	May 15	37°59.0	7°58.6	19.0	2770	64	29 <mark>,</mark> 2	182	66	 Supprimé: ,
	ST5	May 16	38°57.2	11°1.4	19.5	2366	77	30 <u>.</u> 5	148	51	 Supprimé: ,
	TYR	May 17-20	39°20.4	12°35.56	19.6	3395	80 ± 6	29 ± 3	170 ± 35	57 ± 3	
	ST6	May 22	38°48.47	14°29.97	20.0	2275	80	18,7	142	62	 Supprimé: ,
	ST7	May 24	36°39.5	18°09.3	20.6	3627	87	24.2	158	57	
	ION	May 25-28	35°29.1	19°47.77	20.6	3054	97 ± 5	29 ± 2	208 ± 15	51 ± 9	
	ST8	May 30	36°12.6	16°37.5	20.8	3314	94	31.6	206	71	
	ST9	June 2	38°08.1	5°50.5	21.2	2837	91	36.1	214	64	
	FAST	June 2-7 and 9	37°56.8	2°54.6	21.0	2775	79 ± 8	34 ± 8	211 ± 57	92 ± 11	
	ST10	June 8	37°27.58	1°34.0	21.6	2770	89	28 . 9	nd	96	 Supprimé: ,

1595 Table 2. N budget at the short stations within the surface mixed layer (ML). Integrated stocks (NO3, µmol N m⁻²) and fluxes (heterotrophic prokaryotic N demand (hprokN demand), phytoplankton N demand (phytoN demand), in situ leucine aminopeptidase hydrolysis fluxes (LAP), dry atmospheric deposition of NO3 and NH4 (all fluxes in µmol N m⁻² d⁻¹). Values presented as mean ± sd. SD was calculated using propagation of errors: For hprokN demand triplicate measurements at each depth and a C/N ratio of 7.3 ± 1.6; for phytoN demand triplicate measurements of PP at each depth and a C/N ratio of 7 ± 1.4 ; for LAP the analytical TAA error and the Vm and Km errors; for N2fix the coefficient of variation was 10% for volumetric fluxes > 0.1 nmole N $l^{-1} d^{-1}$ and 20% for lower values. For dry deposition, sd is based on the variability of the NO3 and NH4 concentrations solubilized from aerosols during the occupation of the station (see methods section 2.2.1). MLD: mixed layer depth. na: not available because under LWCC detection limits.

		stocks		biological	Dry deposition			
stations	MLD	NO3	phytoN demand	hprokN demand	LAP	N ₂ fixation	NO3	NH4
	m	µmol N m ⁻²	$\begin{array}{c} \mu mol \; N \; m^{-2} \\ d^{-1} \end{array}$		µmol N m ⁻² d ⁻¹			µmol N m ⁻² d ⁻¹
ST1	21	na	1468 ± 325	184 ± 40	121 ± 28	14.6 ± 1.5	18.6 ± 1.4	1.5 ± 0.3
ST2	21	na	481 ± 161	163 ± 35	48 ± 24	10.7 ± 1.1	23.7 ± 2.2	4.1 ± 0.9
ST3	11	na	282 ± 82	126 ± 28	40 ± 17	7.8 ± 0.8	33.8 ± 3.6	4.7 ± 0.5
ST4	15	na	246 ± 80	132 ± 28	83 ± 20	10.7 ± 1.1	23.8 ± 2.9	6.3 ± 2.6
ST5	9	261 ± 22	112 ± 29	42 ± 9	17 ± 12	4.8 ± 0.5	27.0 ± 7.5	7.9 ± 1.8
ST6	18	162 ± 14	410 ± 116	204 ± 44	48 ± 24	9.1 ± 0.9	15.0 ± 0.6	9.3 ± 0.7
ST7	18	162 ± 14	226 ± 123	148 ± 33	83 ± 18	10.5 ± 1.1	23.6 ± 1.9	8.0 ± 1.2
ST8	14	911 ± 77	274 ± 66	130 ± 33	25 ± 8	4.3 ± 0.5	13.4 ± 1.7	3.8 ± 0.6
ST9	7	819 ± 70	259 ± 70	85 ± 22	21 ± 6	3.4 ± 0.4	27.4 ± 3.8	13.5 ± 0.8
ST10	19	2074 ± 176	495 ± 31	294 ± 64	42 ± 26	13.6 ± 1.4	23.9 ± 3.4	4.1 ± 0.4

Table 3. Characteristics and nutrient fluxes estimated in the 2 rain_samples collected during the PEACETIME cruise at ION and FAST sites.

event	Rain ION	Rain FAST
Date and local time	29/05 05:08-6:00	05/06 02:36-3:04
Estimated precipitation (mm)	3.5 ± 1.2	5.7 ± 1.4
DIP Flux nmol P m ⁻²	663 ± 227	1146 ± 290
DOP Flux nmol P m ⁻²	974 ± 334	908 ± 230
POP fluxes nmol P m ⁻²	239 ± 82	8801 ± 2227
NO3 Flux µmol N m ⁻²	67 ± 22	341 ± 86
NH4 Flux µmol N m ⁻²	71 ± 24	208 ± 53
DIN Flux µmol N m ⁻²	138 ± 47	550 ± 139

1615 Figure legends

Figure 1. Nitrate (NO3) aerosol concentration along the PEACETIME transect. The locations of two rain events are indicated by large black circles. Stations ST 1 to 4 were not sampled for nutrient analysis at a nanomolar level.

Figure 2. Representation of the mixed layer (ML), the bottom of the nitrate (NO3) depleted layer (NDLb), delineated by the nitracline depth and the mixed layer depth (MLD).

Figure 3. a) Evolution of the wind speed during the PEACETIME cruise. The stations are indicated in yellow and dates in black. Vertical dotted lines delineate the beginning and the end of the ship's depolyment at TYR, ION and FAST sites. The two rain events collected on board are indicated in solid vertical red arrows and surrounding observed rain events by

horizontal dashed red arrows. b) 0-100 m vertical distribution of nitrate (NO3) with depth.The MLD (in red) and nitracline (in brown) are indicated.

Figure 4. Average concentration of nitrate (NO3) in the ML and the NDLb, and NO3 flux from the ML to NDLb. The stations have been classified into 4 types (1 in blue, 2 in green, 3 in yellow, 4 in red, see section Results and Table S1 for definitions). Error bars are indicated
by standard deviation around average values for nitrate concentrations, and error propagation for the flux from ML to NDLb using a 0.5 m uncertainty in the MLD variation.

Figure 5. Evolution within the ML of heterotrophic prokaryotic production (BP), particulate primary production (PP), heterotrophic prokaryotes (hprok) and *Synechococcus* (syn) abundances at the FAST site. The mixed layer depth is indicated by a red line.

1635

Figure 6. Synthetic view of biogeochemical processes and exchanges between the ML and NDLb at the FAST site before the rain and evolution after the rain.